Bis(alkylguanidinium) Receptors for Phosphodiesters: Effect of Counterions, Solvent Mixtures, and Cavity Flexibility on Complexation

Diane M. Kneeland, Katsuhiko Ariga, Vincent M. Lynch, Chia-Yu Huang, and Eric V. Anslyn*

Contribution from the Department of Chemistry and Biochemistry, The University of Texas at Austin, Austin, Texas 78712-1167

Received April 26, 1993®

Abstract: Four bis(guanidinium) receptors have been synthesized in which the guanidinium groups are spatially preorganized by an octahydroacridine (*meso*-**3** and *d,l*-**3**) or hexahydrodicyclopenta[*b,e*]pyridine (*meso*-**4** and *d,l*-**4**) spacer to complement a phosphodiester. These structures are designed to mimic the active site of staphylococcal nuclease and, thereby, form four hydrogen bonds to a bound phosphodiester with little reorganization of the host structures. The syntheses involve two parts: construction of the spacer and formation of the aminoimidazoline groups via an intramolecular cyclization between an amine and a thiouronium salt. Binding constants between the receptors and dibenzyl phosphate range from 4.0×10^3 to 10 M^{-1} in highly competitive solvent systems such as aqueous DMSO. Each receptor forms both a 1:1 and 2:1 phosphate to host complex. The methods for determining K_1 and K_2 are discussed in detail and involve both ^{31}P and ^1H NMR titration experiments followed by a linear treatment of the data. Binding in pure DMSO is worth 3–4 kcal/mol, but the addition of water significantly decreases the degree of complexation. When the guanidinium counterions are tetraphenylboron, the *meso* forms of the hosts are the best receptors due to preorganization of the guanidinium groups on the same face of the spacer. When the counterions are chloride, the *d,l* forms can be the best receptors due to a specific ion effect where a chloride is involved in the host–guest complex. Addition of chloride salts increases binding, possibly due to a chaotropic "salting-out" phenomenon. The structures of the host–guest complexes of *meso*-**4** with dibenzyl phosphate and phenyl phosphate have been determined by X-ray analysis. The structures demonstrate the chloride-counter ion assistance and confirm the four hydrogen bonds between the host and the guest. Near-identical structures to the crystal structures are calculated by molecular mechanics for the complex formed between dimethyl phosphate and *meso*-**3** and *meso*-**4**. *meso*-**3** has been found to act as an RNA hydrolysis catalyst and is the first step toward the optimization of a functional RNA-cleaving artificial enzyme.

Introduction

The starting point for the design of an artificial enzyme is often the examination of the active site of a natural enzyme. The active site of staphylococcal nuclease (SNase), a DNA- and RNA-hydrolyzing enzyme, has several functional groups which contribute to catalysis.[1] Among these are two guanidinium side chains on arginines-35 and -87, a carboxylate of glutamate-43, and a calcium ion. The mechanism of catalysis and the energetic contribution from each of these functional groups have been studied in detail by single[2] and double-site-directed[3] mutants. The guanidiniums are postulated to orient the substrate via two-point hydrogen bonding and to act as general acids to assist in charge neutralization and leaving-group protonation.[4] The guanidiniums are responsible for $10^{4.6}$-fold out of the total 10^{16}-fold DNA hydrolysis rate enhancement.[2,3] Guanindinium groups are also known to bind phosphates in other phosphatase enzymes,[5] and several synthetic monoguanidinium[6] and diguanidinium[7] hosts have been developed to study such complexation.

In 1992 and 1993, three independent research groups synthesized artificial enzymes that possess two guanidinium-like moieties in an attempt to electrophilically activate phosphate linkages and thereby achieve a fraction of the rate enhancement imparted by the two arginines of SNase. Göbel reported that compound **1** increased the cleavage of a strained phosphodiester in DMF by a factor of 2000-fold.[8] Hamilton reported that compound **2** increased the lutidine-catalyzed transesterification of a *p*-nitrophenyl-activated RNA analog by nearly 1000-fold in acetonitrile,[9] and we reported that compound *meso*-**3** at micromolar concentrations increased imidazole-catalyzed mRNA hydrolysis rates by 20-fold in water.[10] Thus, mimicking the two arginine groups of SNase is a successful strategy for enhancing the rate of phosphodiester P–O bond cleavage under a variety of conditions.

The success of these bis(guanidinium)-SNase mimics resides in an initial binding of the monoanionic tetrahedral phosphodiester substrate followed by an increased electrostatic attraction with

* Abstract published in *Advance ACS Abstracts,* October 1, 1993.

(1) (a) Anfinsen, C. B. *Science* (*Washington, DC*) **1973**, *181*, 223–230. (b) Tucker, P. W.; Hazen, E. E., Jr.; Cotton, F. A. *Mol. Cell. Biochem.* **1979**, *23*, 67–86.

(2) Serpersu, E. H.; Shortle, D.; Mildvan, A. S. *Biochemistry* **1987**, *26*, 1289–1300.

(3) Weber, D. J.; Sepersu, E. H.; Shortle, D.; Mildvan, A. S. *Biochemistry* **1990**, *29*, 8632–8642.

(4) Hannon, C.; Anslyn, E. V. The Guanidinium Group: Its Biological Role and Synthetic Analogs. *Bioorganic Chemistry Frontiers*; Schmitdchen, F., Ed.; in press.

(5) Kim, E. E.; Wycoff, H. W. *J. Mol. Biol.* **1991**, *218*, 449. Schinzel, R.; Drueckes, P. *FEBS Lett.* **1991**, *286*, 125.

(6) Muller, G.; Riede, J.; Schmidtchen, F. P. *Angew. Chem., Int. Ed. Engl.* **1988**, *27*, 1516–1518. Echavarren, A.; Galan, A.; de Mendoza, J.; Salmeron, A.; Lehn, J.-M. *Helv. Chim. Acta* **1988**, *71*, 685–693. Echavarren, A.; Galan, A.; Lehn, J.-M.; de Mendoza, J. *J. Am. Chem. Soc.* **1989**, *111*, 4994–4995. Schmidtchen, F. P.; Gleich, A.; Schummer, A. *Pure Appl. Chem.* **1989**, *61*, 1535–1546. Gleich, A.; Schmidtchen, F. P.; Mikulcik, P.; Müller, G. *J. Chem. Soc., Chem. Commun.* **1990**, 55–57. Kurzmeier, H.; Schmidtchen, F. P. *J. Org. Chem.* **1990**, *55*, 3749–3755. Galan, A.; Pueyo, E.; Salmeron, A.; de Mendoza, J. *Tetrahedron Lett.* **1991**, *32*, 1827–1880. Galan, A.; de Mendoza, J.; Toiron, C.; Bruix, M.; Deslongchamps, G.; Rebek, J., Jr. *J. Am. Chem. Soc.* **1991**, *113*, 9424–9425. Galan, A.; Andreu, D.; Echavarren, A. M.; Prados, P.; de Mendoza, J. *J. Am. Chem. Soc.* **1992**, *114*, 1511–1512.

(7) Dietrich, B.; Fyles, T. M.; Lehn, J.-M.; Pease, L. G.; Fyles, D. L. *J. Chem. Soc., Chem. Commun.* **1978**, 934–936. Dietrich, B.; Fyles, D. L.; Fyles, T. M.; Lehn, J.-M. *Helv. Chim. Acta* **1979**, *62*, 2763–2787. Schmidtchen, F. P. *Tetrahedron Lett.* **1989**, *30*, 4493.

(8) Göbel, M. W.; Bats, J. W.; Durner, G. *Angew. Chem., Int. Ed. Engl.* **1992**, *31*, 207–209.

(9) Jubian, V.; Dixon, R. P.; Hamilton, A. D. *J. Am. Chem. Soc.* **1992**, *114*, 1120–1121.

(10) Smith, J.; Ariga, K.; Anslyn, E. V. *J. Am. Chem. Soc.* **1993**, *115*, 362–364.

0002-7863/93/1515-10042$04.00/0

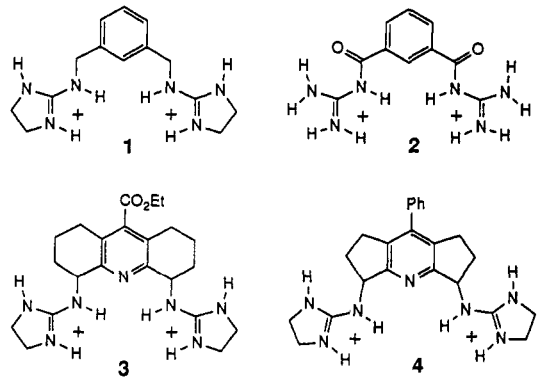

the dianionic trigonal bipyramidal phosphorane transition state.[11] The initial complexation in aqueous media is quite difficult due to competition with the water solvating the guanidinium groups and the phosphate substrate.[12] Since catalysis starts with substrate binding but aqueous media is highly competitive, our initial efforts were focused on maximizing the preorganization and the complementarity of bis(guanidinium) receptors for phospho diester substrates in order to maximize complexation.[13] Herein, the effects of cavity flexibility, of hydrogen-bonding solvents, and of guanidinium counterions upon complexation strength are discussed.

Results and Discussion

Design Criteria. The design of receptors **3** and **4** has, as its starting point, the crystal structure of SNase with 3′,5′-thymidine diphosphate (pdTp), performed by Cotton.[14] Figure 1A is a schematic representation of the position of the catalytic groups found in this crystal structure. Of interest to this work are the two guanidiniums, each of which makes two hydrogen bonds to the dianionic phospho monoester pdTp. Cotton also found that the simple compounds methylguanidinium dihydrogen phosphate[15] and bis(methylguanidinium) monohydrogen phosphate[16] both crystallize to form a similar hydrogen-bonding pattern (Figure 1B). Even in these simple structures, each guanidinium forms two hydrogen bonds to the phosphoric acid moiety. Thus, we reasoned that a design using two guanidiniums in the manner shown in Figure 2 would lead to a successful phospho diester receptor and a possible hydrolysis catalyst.[10]

The spacer between the two guanidiniums was designed to converge the hydrogen-bonding groups to complement a bound phospho diester without significant reorganization of the receptor. An octahydroacridine spacer was chosen on the basis of the literature precedent with isophthaloyl spacers.[17] These spacers, when incorporated in a macrocycle, properly orient hydrogen-bonding groups for complexation of structures such as barbiturates.[17] In contrast to an isophthaloyl spacer, however, an octahydroacridine spacer holds the guanidinium groups preorganized and converged without using a macrocycle. Such preorganization has been found to be crucial in "molecular tweezers".[18] In addition, preorganization should lead to a greater tendency for the guanidiniums to bind only one phosphate along a polyphosphate chain as in RNA or DNA. Octahydroacridine was used instead of acridine because of the basicity difference between bis(alkylguanidinium) groups versus that of bis(arylguanidinium) groups. Alkylguanidiniums are desirable for catalytic studies in water because their pK_as (near 13)[19] allow them to remain protonated over a wider pH range than those of arylguanidiniums (pK_as near 9–10).[20] Finally, instead of attaching the parent guanidinium group (with all hydrogens on the nitrogens) to the spacers, aminoimidazoline groups were chosen. The two-point hydrogen-bonding capabilities are the same as those for guanidiniums, and their pK_as are similar, but the methylenes block hydrogen-bonding sites, thereby preventing multiple association like that found in similar systems.[21]

In addition to examining an octahydroacridine spacer in **3**, a hexahydrodicyclopenta[*b*,*e*]pyridine spacer in **4** was explored.

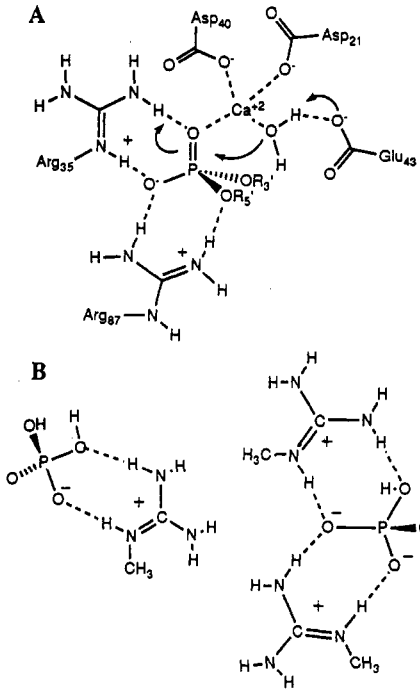

Figure 1. (A) Schematic representation of the staphylococcal nuclease active site. (B) Simple guanidinium phosphate salt structures.

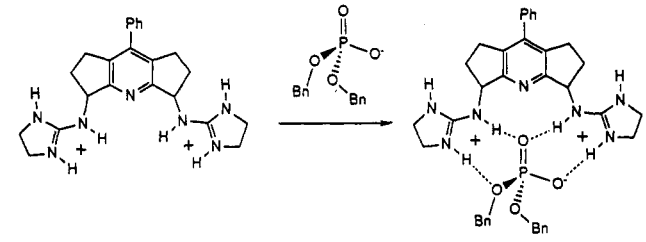

Figure 2. Idealized four-point hydrogen-bonding complexation geometry for bis(guanidinium) receptors with dibenzyl phosphate.

(11) Postulate is based upon the following: Fersht, A. *Enzyme Structure and Mechanism*, 2nd ed; W. H. Freeman and Co.: New York; Chapter 12.

(12) For other hydrogen-bonding complexation in mildly to highly competitive solvents, see: Constant, J. F.; Fahy, J.; Lhomme, J. *Tetrahedron Lett.* **1987**, *28*, 1777–1780. Furuta, H.; Magda, D.; Sessler, J. L. *J. Am. Chem. Soc.* **1991**, *113*, 978–985. Kelly-Rowley, A. M.; Cabell, L. A.; Anslyn, E. V. *J. Am. Chem. Soc.* **1991**, *113*, 9687–9688. Fan, E.; Van Arman, S. A.; Kincaid, S.; Hamilton, A. D. *J. Am. Chem. Soc.* **1993**, *115*, 369–370. Rotello, V. M.; Viani, E. A.; Deslongchamps, G.; Murray, B. A.; Rebek, J., Jr. *J. Am. Chem. Soc.* **1993**, *115*, 797–798.

(13) Ariga, K.; Anslyn, E. V. *J. Org. Chem.* **1992**, *57*, 417–419.

(14) Cotton, F. A.; Hazen, E. E., Jr.; Legg, M. J. *Proc. Natl. Acad. Sci. U.S.A.* **1979**, *76*, 2551–2555.

(15) Cotton, F. A.; Day, V. W.; Hazen, E. E., Jr.; Larsen, S. *J. Am. Chem. Soc.* **1973**, *95*, 4834–4840.

(16) Cotton, F. A.; Day, V. W.; Hazen, E. E., Jr.; Larsen, S.; Wong, S. T. K. *J. Am. Chem. Soc.* **1974**, *96*, 4471–4478.

(17) For isophthaloyl spacers, see: Goswami, S.; Hamilton, A. D. *J. Am. Chem. Soc.* **1989**, *111*, 3425–3426. Hamilton, A. D. *J. Chem. Educ.* **1990**, *67*, 821–828. Tecilla, P.; Chang, S. K.; Hamilton, A. D. *J. Am. Chem. Soc.* **1990**, *112*, 9586–9590. Chang, S. K.; Van Engen, D.; Fan, E.; Hamilton, A. D. *J. Am. Chem. Soc.* **1991**, *113*, 7640–7645. Kluger, R.; Tsao, B. *J. Am. Chem. Soc.* **1993**, *115*, 2089–2090.

(18) Zimmerman, S. C.; Mrksich, M.; Baloga, M. *J. Am. Chem. Soc.* **1989**, *111*, 8528–8530.

(19) Dean, J. A. *Lange's Handbook of Chemistry*, 13th ed.; Mc-Graw Hill Book Co.: New York, 1985. Angyal, S. J.; Warburton, W. K. *J. Chem. Soc.* **1951**, 2492–2494.

(20) Perrin, D. D. *Dissociation Constants of Organic Bases in Aqueous Solution*; Butterworths: London, 1965.

(21) Dixon, R. P.; Geib, S. J.; Hamilton, A. D. *J. Am. Chem. Soc.* **1992**, *114*, 365–366.

Scheme I. Module 1, Synthetic Routes to Spacers **5** and **6**

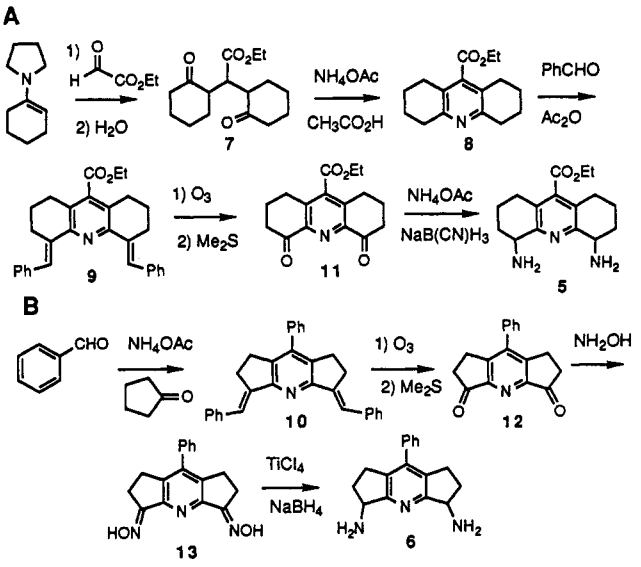

The goal of this change was to examine binding characteristics as the angle and the rigidity between the aminoimidazolines changed with other characteristics of the receptor remaining the same. The angle between and the rigidity of the guanidinium groups are related to puckering of the cyclohexeno or cyclopenteno rings in **3** and **4**. The cyclopenteno rings allow envelope-type puckering modes, whereas the cyclohexeno rings of **3** allow for each guanidinium group to be either axial or equatorial.

Synthesis. For kinetic studies on phosphodiester hydrolysis, fairly large quantities of the catalysts will be required. In addition, studies of the effects of different spatial positions of the guanidinium groups upon catalysis and the addition of more functional groups require a versatile synthesis. The synthesis involved two parts: the spacer and the aminoimidazolines. The *meso* and *d,l* forms of receptors **3** and **4** can be typically prepared on 1.5–3-g scales.

The syntheses of **3** and **4** focus initially upon constructing the rigid spacers **5** and **6** that hold the aminoimidazoline groups at specific distances and angles (Scheme I). The routes to diamines **5** and **6** are quite versatile in the sense that many different groups can be placed in the para position of the central pyridine and because the receptor size can be changed by using either cyclohexanone or cyclopentanone. The former allows for future functionalization while the latter allows for a subtle change in cavity size. The synthetic routes to these spacers are based upon extensive work from the Thummel[22] and Bell groups.[23]

The synthesis of **5** began with an enamine condensation of cyclohexanone with ethyl glyoxylate to form **7** followed by a reflux with ammonium acetate in acetic acid that afforded octahydroacridine **8**. Activation of the benzylic positions was effected by refluxing **8** in acetic anhydride with benzaldehyde. Less than refluxing temperature resulted in the isolation of some monoactivated benzylic position with *Z*-double bond stereochemistry, thus blocking a second benzaldehyde addition. The product **9** was isolated by vacuum distillation of the solvent and excess benzaldehyde and crystallization from ethyl acetate to form large yellow plates. The overall yield for the three steps was typically near 25%. In contrast, these three steps can be combined in a one-pot reaction in the synthesis of **6**. Refluxing benzaldehyde, cyclopentanone, and ammonium acetate in ethanol for approximately 1 h formed a yellow crystalline precipitate of crude **10**. After recrystallization from ethyl acetate, **10** was also isolated in 25% yield.[24]

From the point of isolating **9** and **10**, the syntheses of **3** and **4** only differ in the method of transforming diketones **11** and **12** to diamines **5** and **6**. Both compounds **9** and **10** undergo smooth ozonolysis followed by reductive workup to form diketones **11** and **12**. Compound **11** undergoes efficient reductive amination under the typical conditions[25] to form diamine **5**. In contrast, diketone **12** when subjected to ammonium acetate and $NaB(CN)H_3$ immediately turns black, and none of **6** can be isolated. Rather than pursuing other reductive amination conditions for transforming **12** to **6**, a two-step method involving the intermediate dioxime **13** was utilized. Compound **13** was easily isolated by collection of the cream-colored precipitate formed upon warming **12**, Na_2CO_3, and $NH_2OH{\cdot}HCl$ in DMF. Treatment of **13** with $NaBH_4$ and $TiCl_4$ in dry DME[26] effected the reduction to **6** in 50% yield.

The method of separation of the *meso* and *d,l* isomers of **5** and **6** is outlined in Scheme II. The *meso* and *d,l* isomers of both **5** and **6** can be observed to separate on a silica plate with 15% ammonia-saturated methanol in ethyl acetate eluent, but preparative flash chromatography proved difficult due to extensive streaking. On the basis of the assumption that the streaking was due to the highly polar nature of the diamines, a method involving a less polar derivative was pursued. The reaction of **5** and **6** with di-*tert*-butyl dicarbonate in chloroform cleanly gave **14** and **15**, from which the *meso* and *d,l* forms could be easily separated by flash chromatography on silica gel with 50/50 ethyl acetate/hexanes eluent, the *d,l* isomer eluting first. Clean removal of the tBoc groups was accomplished by standard methods to yield the separated *d,l* and *meso* isomers of **5** and **6** in nearly quantitative yields.

The isomers were identified by X-ray crystal structures (as discussed below) for compound **4**, but the ^1H NMR of the *meso* and *d,l* isomers of **5** revealed the appropriate stereochemistry of **3**. Figure 3 displays the 500-MHz ^1H NMR spectra of the CH_2 moiety of the ethyl ester in both the *meso* and *d,l* forms of **5**. In the *meso* form, the CH_2 group is not diastereotopic and the resonance is a clean quartet. In contrast, the CH_2 group in the *d,l* form is diastereotopic. The diastereotopic protons form an AB pattern that is further split by the methyl group to give a possible 16-line pattern. Only 12 lines are found due to coincidental overlap.

Formation of the aminoimidazoline groups employed an intramolecular five-membered-ring cyclization between an amine and a thiouronium salt (Scheme III) similar to intermolecular procedures.[27] This four-step route was adopted since the reaction of **5** or **6** with 2-(methylthio)-2-imidazoline (which would yield **3** and **4** directly) resulted in exceptionally low yields. The new aminoimidazoline-forming procedure centers around the synthesis of **16**, which couples easily with amines to form thioureas. Compound **16** was synthesized by the monoprotection of ethylenediamine by di-*tert*-butyl dicarbonate followed by treatment with carbon disulfide and DCC.[28] The reaction of **5** and **6** with **16** gave high yields of **17** and **18**, respectively. *S*-Alkylation of **17** and **18** followed by deprotection and base-mediated cyclization afforded **3** and **4**, respectively, both in near 36% overall yield from their respective precursors **5** or **6**. Purification of the free bases **3** and **4** proceeded by silica gel chromatography followed by formation of bis(picrate) salts. The picrates could be converted

(22) Thummel, R. P.; Jahng, Y. *J. Org. Chem.* **1985**, *50*, 2407–2412. Thummel, R. P.; Hedge, V. *J. Org. Chem.* **1989**, *54*, 1720–1725. Thummel, R. P. *Tetrahedron* **1991**, *47*, 6851–6886. Hedge, V.; Hung, C.-Y.; Madhukar, P.; Cunningham, R.; Hopfner, T.; Thummel, R. P. *J. Am. Chem. Soc.* **1993**, *115*, 872.

(23) Bell, T. W.; Liu, J. *J. Am. Chem. Soc.* **1988**, *110*, 3673–3674. Bell, T. W.; Liu, J. *Angew. Chem., Int. Engl.* **1990**, *29*, 923–925.

(24) Baliah, V.; Jeyaraman, R. *Ind. J. Chem.* **1977**, *15B*, 798–799.

(25) Borch, R. F.; Bernstein, M. D.; Durst, H. D. *J. Am. Chem. Soc.* **1971**, *93*, 2897.

(26) Kano, S.; Tanaka, Y.; Sugino, E.; Satsoshi, H. *Synthesis* **1980**, 695.

(27) Bello, J. *Biochim. Biophys. Acta* **1955**, *18*, 448. Heyboer, N.; Heymans, V.; Visser, G.; Kerling, K. E. T. *Recl. Trav. Chim. Pays-Bas* **1962**, *81*, 69–72. Also see reference 8.

(28) Jochims, J. C.; Seeliger, A. *Angew. Chem., Int. Ed. Engl.* **1967**, *6*, 174–175.

Scheme II. Strategy for Separation of the *meso* and *d,l* Isomers of **5** and **6**

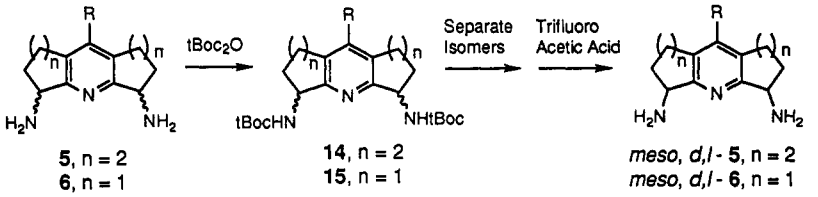

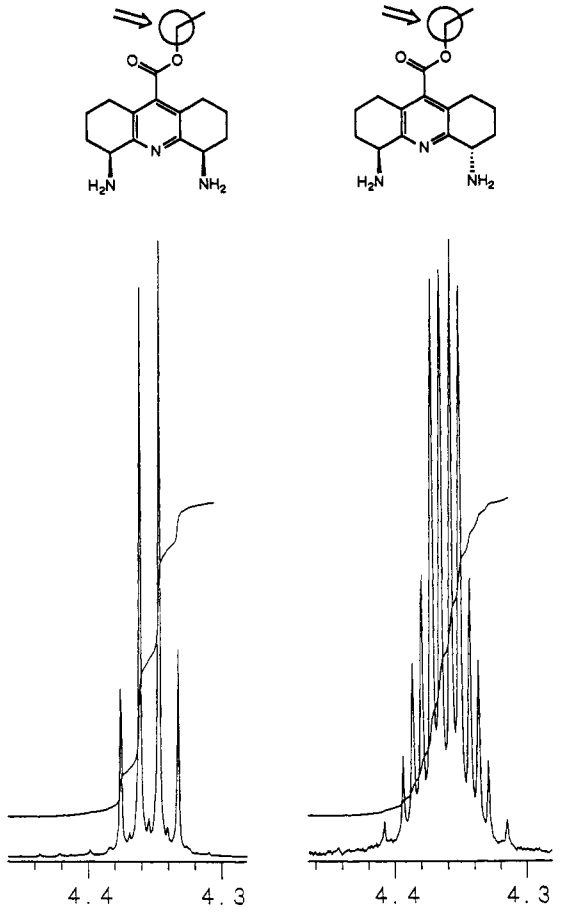

Figure 3. ^1H NMR spectra of the methylene ethyl hydrogens of *meso*-**5** and *d,l*-**5**.

to chlorides by anion-exchange chromatography, and the chlorides could be converted to tetraphenylborates by a metathesis with sodium tetraphenylborate in acetonitrile or water.

Complexation Studies. Methods. The binding constants between receptors **3** and **4** were primarily determined from ^{31}P NMR titrations. The dibenzyl phosphate concentration was held constant, and the concentration of the receptor was incrementally changed to span a host to guest ratio between 0 and 6. In low percentages of H_2O in DMSO, curves were generated that indicated 1:1 and 2:1 phosphate (P) to host (H) complex formation. As water percentages approached and exceeded 20, only 1:1 phosphate to host complexation was observed. Two representative binding isotherms are shown in Figure 4. The inflections in the isotherms are indicative of the two equilibria shown in eq 1. Since

$$H + P \underset{}{\overset{K_1}{\rightleftharpoons}} HP \qquad HP + P \overset{K_2}{\rightleftharpoons} HP_2 \qquad (1)$$

the isotherms begin with dibenzyl phosphate in excess, the first complex is HP_2 which exists in highest concentration near 0.5 equiv of host. As the host concentration increases, the equilibria shift to predominately the HP complex. Thus, the initial rise in the chemical shift represents formation of the HP_2 complex, and the plateau in the chemical shift near the end of the isotherm represents the ^{31}P NMR resonance of the HP complex.

Fitting such curves to a two-equilibria expression is complicated by the fact that there are five variables: two binding constants (K_1 and K_2) and three NMR resonances (free phosphate, δ_P; 1:1 phosphate–host complex, δ_{HP}; and 2:1 phosphate–host complex, δ_{HP_2}). In all of the studies, the free-phosphate ^{31}P NMR chemical shift was determined independently. The ^{31}P NMR chemical shift of HP could typically be determined to within 0.5 ppm by inspection of the binding isotherm since saturation binding was nearly always achieved. Thus, the variables were reduced to three: the two binding constants and the HP_2 chemical shift.

A method for determining 1:1 and 2:1 complexation constants from NMR data when following the chemical shift of the species whose stoichiometry is two in the 2:1 complex has been discussed.[29] We used a similar but slightly modified procedure. Equation 2

$$\delta_{obs} = ([P]/[P]_0)\delta_P + ([HP]/[P]_0)\delta_{HP} + 2([HP_2]/[P]_0)\delta_{HP_2} \qquad (2)$$

shows the relationship of the observed chemical shift to the concentration of the complexes in solution where $[P]_0$ is the total phosphate concentration. If one solves for [P] from the K_1 and K_2 equilibria expressions as a function of total host $[H]_0$ and total phosphate $[P]_0$, eq 3 is obtained.[29] Equations 4 and 5 give [HP]

$$K_1K_2[P]^3 + K_1(2K_2[H]_0 - K_2[P]_0 + 1)[P]^2 + (K_1[H]_0 - K_1[P]_0 + 1)[P] - [P]_0 = 0 \qquad (3)$$

$$[HP] = K_1[H]_0[P]/(K_1K_2[P]^2 + K_1[P] + 1) \qquad (4)$$

$$[HP_2] = K_1K_2[H]_0[P]^2/(K_1K_2[P]^2 + K_1[P] + 1) \qquad (5)$$

and $[HP_2]$, respectively, as a function of [P]. The cubic eq 3 was solved by the Newton–Raphson technique for multiple $[H]_0$s and with several initial estimates of K_1 and K_2. Each [P] solved for from eq 3 was used to solve eqs 4 and 5. The resultant [P], [HP], and $[HP_2]$ were substituted into eq 2. The variables K_1, K_2, and δ_{HP_2} were visually changed to optimize the theoretical fit to the data. It was found that the use of a nonlinear least-squares fitting routine based upon the simplex algorithm[30] did not give significantly different results than those from a visual fit.

The HP_2 complex under all our experimental conditions possessed a lower field chemical shift than free dibenzyl phosphate, whereas the 1:1 complex possessed a higher field chemical shift. Figure 5 and 6 show theoretically generated ^{31}P NMR binding isotherms generated by the method discussed above. In Figure 5, the chemical shifts of P, HP, and HP_2 are held constant while

(29) Lenkinski, R. E.; Elgavish, G. A.; Reuben, J. *J. Magn. Reson.* **1978**, *32*, 367–376.

(30) Press, W. H.; Flannery, B. P.; Tevkolsky, W. H.; Vetterling, W. T. *Numerical Recipes: The Art of Scientific Computing*; Cambridge, New York. Shavers, C. L.; Parsons, M. L.; Deming, S. N. *J. Chem. Educ.* **1979**, *56*, 307–309.

Scheme III. Module 2, Synthetic Routes for Construction of the Aminoimidazoline Groups

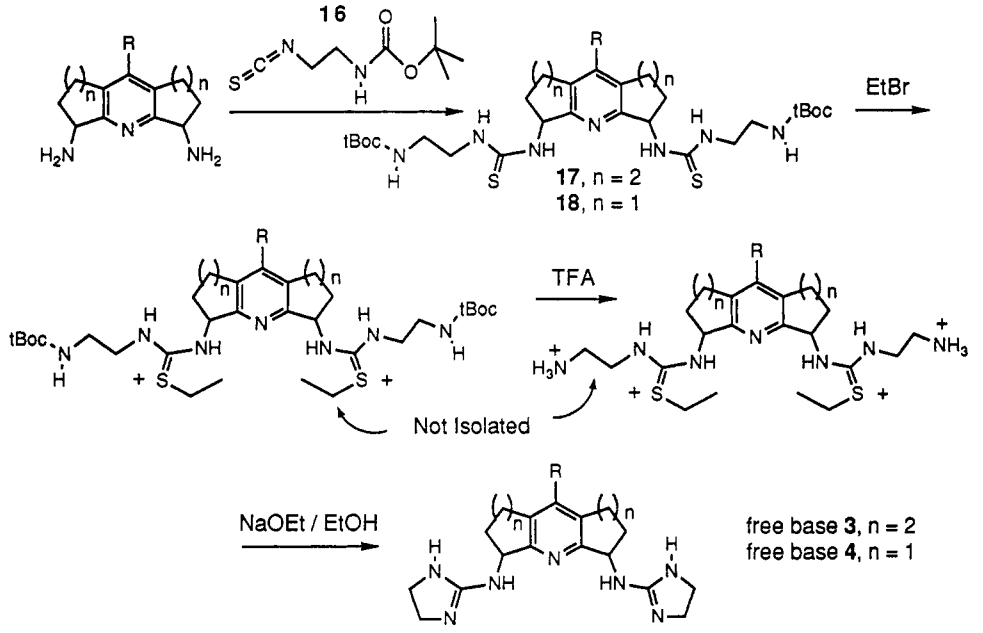

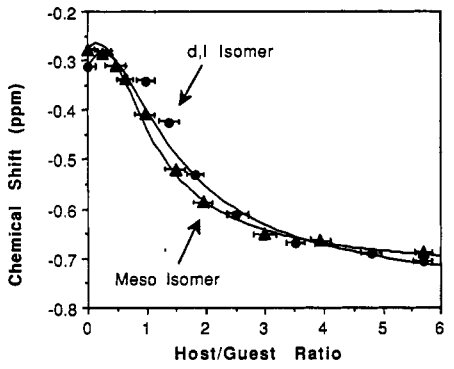

Figure 4. Typical ^{31}P NMR binding isotherms: ▲ = 1.15 × 10^{-2} M dibenzyl phosphate in 15% D_2O/DMSO-d_6 with increasing *meso*-**4** and ● = 8.6 × 10^{-3} M dibenzyl phosphate in 15% D_2O/DMSO-d_6 with increasing *d,l*-**4**. The lines drawn are the calculated fits. The *y*-axis errors represent ±15% estimated error in determining the host/guest ratio. The error in reading the chemical shift is within the size of the marker.

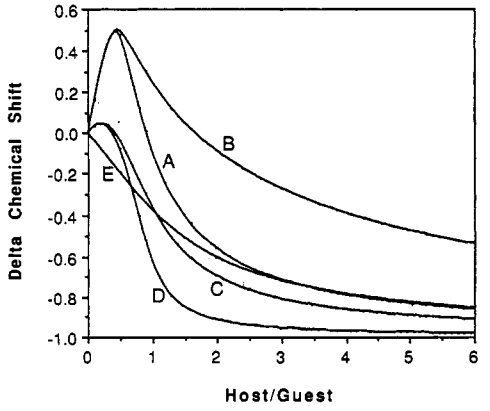

Figure 5. Theoretical ^{31}P NMR binding isotherms. All curves have δ_P = 0 ppm, δ_{HP} = −1 ppm, and δ_{HP_2} = 1 ppm. (A) K_1 = 5000 M^{-1}, K_2 = 1000 M^{-1}; (B) K_1 = 1000 M^{-1}, K_2 = 1000 M^{-1}; (C) K_1 = 1000 M^{-1}, K_2 = 100 M^{-1}; (D) K_1 = 5000 M^{-1}, K_2 = 100 M^{-1}; and (E) K_1 = 200 M^{-1}, K_2 = 20 M^{-1}.

the magnitudes and the ratios of K_1 and K_2 are varied. With line A, both K_1 and K_2 are relatively large and only 5-fold different from each other. This creates a binding isotherm that is slow to

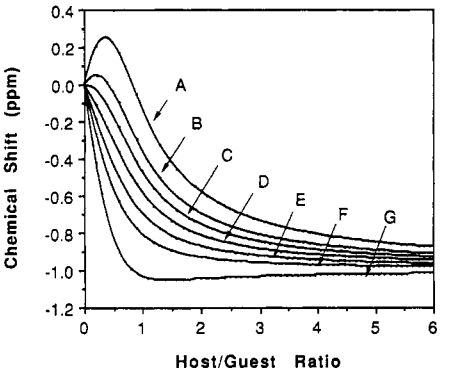

Figure 6. Theoretical ^{31}P NMR binding isotherms. All curves have K_1 = 1000 M^{-1}, K_2 = 400 M^{-1}, δ_{HP} = −1 ppm, and δ_P = 0 ppm. (A) δ_{HP_2} = 2 ppm, (B) δ_{HP_2} = 1 ppm, (C) δ_{HP_2} = 0.5 ppm, (D) δ_{HP_2} = 0 ppm, (E) δ_{HP_2} = −0.5 ppm, (F) δ_{HP_2} = −1 ppm, and (G) δ_{HP_2} = −2 ppm.

plateau as a result of a significant amount of the HP_2 complex being present over a wide range of concentrations. Lines D and E represent ratios of K_1 to K_2 of 10 and 50, respectively, with a relatively low K_2 binding constant. In these cases, there is very little inflection in the isotherms found at 0.5 equiv of host, giving as a result a quick plateau. Thus, visual examination of the experimentally determined isotherms yields insight into the relative ratios of the binding constants. In Figure 6, the magnitudes of K_1, K_2 and δ_{HP} are held constant and δ_{HP_2} is varied. Experimental examples similar to these theoretical curves yield insight into the chemical shifts of HP and HP_2.

Figure 4 shows two representative experimental isotherms (not our best nor our worst matches between experiment and theory) for the *meso* and *d,l* isomers of **4** in 15% aqueous DMSO. The differences in binding characteristics between the two isomers are evident by inspection. The isotherm for the *d,l* isomer shows a downfield shift initially followed by an upfield plateau. In contrast, the isotherm for the *meso* isomer shows a continuous upfield shift. One explanation for the difference between the *meso* and *d,l* isotherms at 0.5 host to guest ratio is that both K_2s are similar but δ_{HP_2}s are different. A confirmation of these chemical shift differences will be discussed with respect to Figure 6. In addition, the curve for the *d,l* isomer is still moving upfield while the curve for the *meso* isomer has nearly reached a plateau at a host to guest ratio of 6. Therefore, K_1 is larger for the *meso*

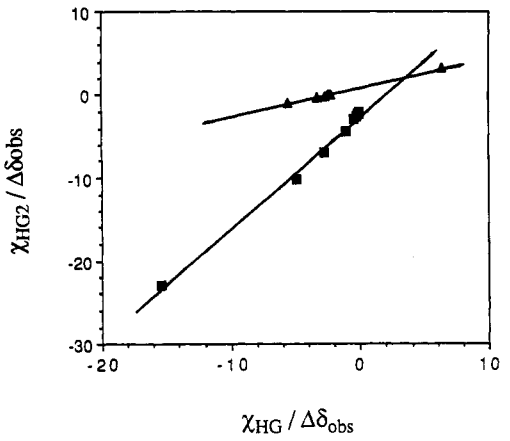

Figure 7. Linear treatment (eq 6) of the experimental data given in Figure 4: ■, data from *meso*-**4**, and ▲, data from *d,l*-**4**.

compound on the basis of the higher extent of saturation at 6 equiv of host. These observations are confirmed by theory which yields K_1 = 550 and 400 M^{-1} for *meso*-**4** and *d,l*-**4**, respectively, and K_2 for both isomers being 40 M^{-1} (Table II).

In all the cases studied, the K_1 binding constant is a reliable value but complications can arise with respect to K_2 when there is no prior knowledge of the magnitude of K_2 and δ_{HP_2}. In these cases, the same experimental binding isotherm can be fit if one K_2 is arbitrarily chosen and the δ_{HP_2} is optimized or vice versa. The isotherms, however, could not be fit with significantly different K_1s. The magnitude of K_2, however, can be determined by a ^1H NMR titration binding experiment.

To confirm the binding constants measured by the ^{31}P NMR technique, several were also measured by ^1H NMR titrations. In Tables I and II (discussed below), the binding constants that were confirmed by ^1H NMR are marked with an asterisk. In these experiments the host concentrations were held constant and either the guanidinium hydrogen resonances or the aminoimidazoline methylene resonances were followed as a function of increasing concentrations of dibenzyl phosphate. The algorithm for fitting a 1:1 and 2:1 NMR isotherm when following the chemical shift of the species whose stoichiometry is one has been discussed.[31] The agreements with the binding constants obtained by the ^1H NMR method were typically within 15% or less of those obtained by the ^{31}P NMR method. The agreement with the ^{31}P NMR data was best for the *meso* forms of **3** and **4**, for which little scatter in the experimental proton data was observed. However, for the *d,l* forms, the chemical shift of the protons changed less and therefore possessed more scatter and the absolute values were not as reliable. However, it is clear that the general trend as measured by ^{31}P NMR is confirmed by the ^1H NMR.

As a further confirmation of the validity of the binding constants reported in Tables I and II, a simple algebraic manipulation of eq 2 can be performed that creates a linear form giving a check on K_1 and K_2.[29] If we define $\Delta\delta$s as the change in chemical shift from that of δ_P and χ as mole fractions, then eq 2 can be transformed to eq 6. Substituting the mole fractions of HP and

$$\underset{b}{(1/\Delta\delta_{HP_2})} - \underset{m}{(\Delta\delta_{HP}/\Delta\delta_{HP_2})}\ \underset{x}{(\chi_{HP}/\Delta\delta_{obs})} = \underset{y}{2(\chi_{HP_2}/\Delta\delta_{obs})} \quad (6)$$

HP_2 (calculated for each $[H]_0$ and $[P]_0$ by using the K_1 and K_2 determined by the Newton–Raphson technique) into eq 6 and plotting $(\chi_{HP}/\Delta\delta_{obs})$ versus $2(\chi_{HP_2}/\Delta\delta_{obs})$ should yield a straight line with $(1/\Delta\delta_{HP_2})$ and $(\Delta\delta_{HP}/\Delta\delta_{HP_2})$ as the intercept and the slope, respectively. Figure 7 shows the results of checking the data from Figure 4. As discussed above, the curves of Figure 4 suggest different δ_{HP_2} values but similar δ_{HP} values. This is confirmed by the fact that the theoretical fit to the experimental curves of Figure 4 yields lines by the eq 6 treatment and that the *y* intercepts representing $(1/\Delta\delta_{HP_2})$ are quite different. Thus, the overall procedure for measuring the binding constants involved independent ^1H and ^{31}P NMR titrations followed by linearizing the ^{31}P NMR data to eq 6.

The binding studies that involved simple one to one complexes were performed by following the ^{31}P NMR dibenzyl phosphate chemical shift as a function of the concentration of various receptors. The data were then fit to the conventional 1:1 binding algorithm that has been previously discussed.[32] On the basis of repetitive measurements of the binding constants by either the ^1H or ^{31}P NMR technique, we estimated at worst a 25% error on all the binding constants reported.

Effect of Host Cavity Size and Counterions. Table I lists the binding constants between the *meso* and *d,l* forms of **3** and **4** with dibenzyl phosphate. In pure DMSO, both hosts show stronger binding in the *meso* form than in the *d,l* form when the counterion is tetraphenylborate. This suggests that the aminoimidazolines are acting cooperatively in the *meso* forms to complex the phosphate and that the cooperativity is at a maximum when the aminoimidazolines are positioned on the same face of the spacer. *meso*-**3** shows stronger binding than *meso*-**4**. This supports a more complementary cavity with **3** than with **4**. We postulate that the octahydroacridine spacer in **3** is more flexible than that in **4** and that this flexibility allows the cavity to adjust to the phosphodiester substrate. The difference, however, between the *meso* forms of **3** and **4** is less than 0.3 kcal/mol, and thus both structures are quite comparable. In contrast, both K_1 and K_2 for the *d,l* form of **4** are similar, indicating that the guanidiniums act independently. Thus, the spacer in **4** does not have enough flexibility to allow the guanidiniums of both the *meso* and *d,l* forms to adopt similar spatial positions when binding a phosphodiester. The *d,l* form of **4** must therefore restrict the aminoimidazoline groups to be on different sides of the spacer and to not be appropriately positioned to act cooperatively to complex the phosphodiester.

The effect of these differences of flexibility and the relative sizes of the binding constants on the ability of these receptors to act as phosphodiester hydrolysis catalysts has not yet been determined. It will be interesting to discover if the more flexible receptors are better catalysts due to better accommodation of the geometry change between tetrahedral substrates and trigonal bipyramidal-like transition states or if the more rigid *meso*-**4** will be better due to a wider cavity that is more complementary to the expanded coordination sphere of the transition state.

Cooperativity for phosphodiester binding between the aminoimidazolines in *meso*-**3** and *meso*-**4** is further supported by comparison with the binding constant of dibenzyl phosphate to **19**. K_1, using either chloride or tetraphenylborate counterions, is 350 M^{-1}. In comparison, compounds **3** and **4** have binding constants greater than that of **19**. This supports the postulate

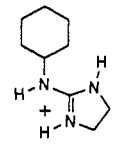

19

that the guanidinium groups of **3** and **4** are acting cooperatively to bind the dibenzyl phosphate guest and that a 0.8–1.1 kcal/mol advantage is gained by preorganizing two guanidiniums in a binding array similar to that of SNase (calculated from the tetraphenylborate salts of **3** and **4**). This energy advantage can result from either a chelation effect due to two additional hydrogen bonds formed from the second guanidinium or binding to one

(31) Friedrichsen, B. P.; Powell, D. R.; Whitlock, H. W. *J. Am. Chem. Soc.* **1990**, *112*, 8931–8941.

(32) Wilcox, C. S.; Cowart, M. D. *Tetrahedron Lett.* **1986**, *27*, 5563–5566.

Table I. K_1 and K_2 Binding Constants for Dibenzyl Phosphate with the Different Isomers of **3** and **4** in DMSO, Solved for by the ^{31}P NMR Titration Method[a]

	compound							
conditions	*meso*-**3**·2Cl⁻	*d,l*-**3**·2Cl⁻	*meso*-**4**·2Cl⁻	*d,l*-**4**·2Cl⁻	*meso*-**3***·2B(Ph)$_4$⁻	*d,l*-**3**·2B(Ph)$_4$⁻	*meso*-**4***·2B(Ph)$_4$⁻	*d,l*-**4***·2B(Ph)$_4$⁻
0% H_2O/100% DMSO	2.2×10^2	2.5×10^3	4.0×10^3	1.0×10^3	2.2×10^3	8.0×10^2	1.4×10^3	9.6×10^2
	1.8×10^2	1.0×10^2	1.0×10^2	4.0×10^2	10	10	30	8.8×10^2

[a] Those entries marked with an asterisk indicate that the binding constants were verified by ^1H NMR titrations. All M^{-1}. Error estimated at 20%.

guanidinium with a neighboring second positive charge. We prefer the former explanation based upon crystal structures and molecular mechanics (discussed below).

The term cooperativity as used above is not meant to imply binding above twice the ΔG value for **19** but only an increase in binding with **3** and **4** compared to that in **19**. The addition of the ΔG for **19** (3.4 kcal/mol) would predict a binding constant of 9.7×10^4 M^{-1} (6.8 kcal/mol) for **3** and **4** in DMSO. Such a large increase, however, is not predicted since the second guanidinium does not form an ion pair with the phosphodiesters as does the first guanidinium. Chelation by the second guanidinium provides only two more hydrogen bonds to the complex. Such hydrogen bonds are not expected to contribute greatly to binding in highly competitive solvents such as DMSO and water, and apparently, the hydrogen bonds increase binding by only about 1 kcal/mol as discussed above. The bis(alkylguanidinium) receptors are, however, designed to achieve a significant chelate effect in the binding of dianionic phosphorane intermediates along the hydrolysis reaction pathway. In contrast to the binding of the monoanionic substrates, catalysis of phosphodiester hydrolysis using receptors **3** and **4** would be expected to benefit from a large increase in binding in the transition state since the phosphorane intermediate is formally minus two and thus a full second ion pair is formed in the transition state that is lacking in the ground state. We are currently working to verify this prediction.

Since both the chloride and the noncoordinating tetraphenylboron salts of **19** bind dibenzyl phosphate similarly in DMSO, the chloride counterion must not compete for complexation with the guanidinium. In contrast, complexation displays unusual results with the chloride salts of the bis(guanidinium) receptors. For the chloride salts, *meso*-**4** binds more strongly than *d,l*-**4** but *d,l*-**3** binds more strongly than *meso*-**3**. This is a different trend than that observed for the tetraphenylborate salts. In addition, the chloride salts of **3** and **4** typically have larger association constants with dibenzyl phosphate than the tetraphenylborate salts. This at first seems counterintuitive since the noncoordinating tetraphenylborates should present no competition in coordinating to the guanidiniums and thus these counterions should yield the largest binding constants for the guanidiniums to the dibenzyl phosphate. The results, however, clearly indicate that the chloride counterion is assisting the phosphodiester binding. As will be discussed below with respect to the effect of added salts and structural studies, the chloride counterion appears to be intimately associated in the 1:1 host to guest complex, yielding a specific ion effect that assists phosphodiester complexation.

Effect of Solvent System. Binding studies between **3** or **4** with dibenzyl phosphate in different ratios of DMSO/water were performed. In percentages of water between 0 and 15, 2:1 binding was observed (Table II). At 20% water, the 2:1 binding vanished and only 1:1 binding was observed which decreased with increasing percentages of water. At 40–50% water, the binding constants became negligible (<10 M^{-1}). Weak binding is, however, still observed for *meso*-**4** (K_1 near 30 M^{-1}) even in 50% H_2O/DMSO. DMSO is a strong hydrogen-bond acceptor and thus competes with the phosphodiester for hydrogen bonding to the hosts,[33] but H_2O is able to solvate both the host and the guest by hydrogen-bond accepting and donating, respectively. In addition, the higher

Table II. K_1 Binding Constants for Dibenzyl Phosphate with the Different Isomers of **3** and **4** (either Cl^- or BPh_4^- counterions) in Various Percentages of D_2O in DMSO-d_6[a]

	compound				
conditions	*meso*-**4**·2Cl⁻	*d,l*-**4**·2Cl⁻	*meso*-**3**·2B(Ph)$_4$	*d,l*-**3**·2B(Ph)$_4$⁻	mix-**3***·2Cl⁻
5% H_2O	2.0×10^3				
	6×10^1				
10% H_2O					3.0×10^2
					6×10^1
15% H_2O	5.5×10^2	4.0×10^2			
	4×10^1	4×10^1			
20% H_2O			7×10^1	1.0×10^2	6×10^1
			7×10^1	1×10^1	2×10^1
25% H_2O	3.3×10^2				
	6.5×10^1				
33% H_2O	6×10^1				3×10^1
50% H_2O	3×10^1				

[a] All M^{-1}. Error estimated at 10–20%.

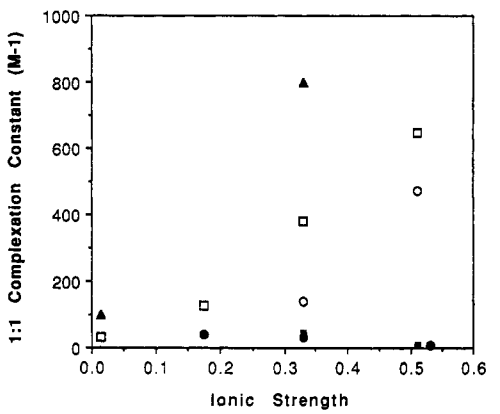

Figure 8. K_1 complexation constants between **3** and dibenzyl phosphate as a function of the ionic strength in (67:33) DMSO/H_2O: ▲ = LiCl, □ = NaCl, ○ = KCl, ■ = $NaClO_4$, and ● = NaSCN.

dielectric effect of water tends to shield the electrostatic attraction of the host and the guest better than that of DMSO.

Effect of Added Salts. Binding studies with a 1:1 mixture of *meso*-**3** and *d,l*-**3** and dibenzyl phosphate were performed with varying ionic strengths. The effect of the ionic strength on the phosphodiester chemical shift was examined prior to this experiment because changes in the ^{31}P NMR chemical shift with ionic strength have been reported.[34] A typical change in ionic strength during a binding study was estimated at ~0.02 M. Chemical shift changes due to this ionic strength change were found to be smaller than 0.012 ppm, which is much smaller than the 1–2 ppm change due to complexation between host and guest.

The results of binding studies with several salts (LiCl, NaCl, KCl, $NaClO_4$, and NaSCN) in DMSO/H_2O (67/33) are shown in Figure 8. All systems showed only 1:1 binding in this high percentage of water. The effect of added salts seemed to be classified into two categories. One category includes LiCl, NaCl, and KCl, which increased the host–guest binding. The other is $NaClO_4$ and NaSCN, which hindered the host–guest binding. These results cannot be interpreted as a dielectric effect because

(33) Lowry, T. H.; Richardson, K. S. *Mechanism and Theory in Organic Chemistry*, 3rd ed.; Harper and Row: Cambridge, 1987; pp 181–189.

(34) Maedritzer, K. *Inorg. Chem.* **1967**, *6*, 936–939. Castello, A. J. R.; Glonek, T.; Van Wazer, J. R. *Inorg. Chem.* **1976**, *15*, 972–974.

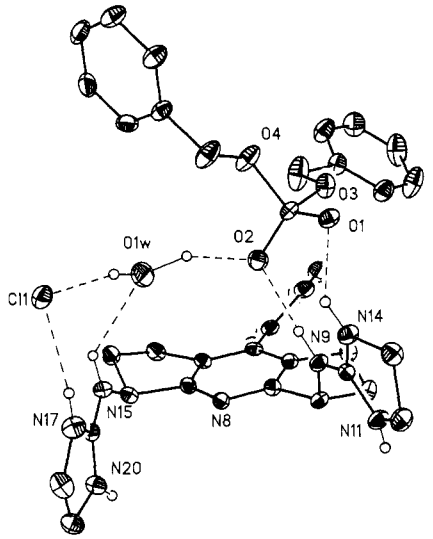

Figure 9. X-ray crystal structure of *meso*-**4** with chloride and dibenzyl phosphate counterions.

an increase in ionic strength should cause a decrease in the electrostatic attractive force between host and guest with all five salts. These results, however, could be interpreted by a salting-in and salting-out chaotropic phenomenon. LiCl, KCl, and NaCl are known as salting-out salts,[35] in which the structure of water is more icelike and therefore a worse solvent for organic groups. In contrast, $NaClO_4$ and NaSCN are known as salting-in salts[35] which destroy the water structure and increase the interaction between organic compounds and water. Evidence for a chaotropic effect on the binding-constant trend is the experimental observation that LiCl increases binding more than NaCl, which in turn increases binding more than KCl. This is the expected trend if the best salting-out compounds would increase binding the most. Chaotropic effects, however, are not the only interactions that lead to increased binding with added chloride salts. Table I shows that the dichloride salts of **3** and **4** bind dibenzyl phosphate better than the tetraphenylborate salts in DMSO. This observation, taken along with the increasing binding constants with increasing NaCl and KCl concentrations, gives evidence that the chloride is part of the 1:1 host to phosphate structure, either coordinated to a guanidinium or in the solvent sphere for charge neutrality. Structure studies (discussed below) support a structure in which the chloride is coordinated to a guanidinium with a water molecule bridging the chloride and the phosphate (Figure 9). The reason for the intimate association of the chloride is the nature of the solvent. DMSO is a good solvator[33] of cations but not of anions, and as a result, association of the chloride to a guanidinium yields charge neutrality as well as hydrogen-bond-donor solvation of the chloride.

Alternatively, chloride may be selectively and preferentially solvated by water, as could Li, Na, and K, thus making the binary solvent system more DMSO-like and increasing the binding constants. Such hetero- and homoselective solvations have been observed previously.[36] Since salting-out phenomenon are typically associated with hydrophobic compounds, however, it is quite interesting to find a trend between the salting-out ability and the aggregation of charges. Clearly this effect deserves further study.

Incorporation of a chloride into the receptor–substrate complex should be detrimental to the catalysis of phosphodiester hydrolysis.

(35) Long, F. A.; McDevit, W. F.; *Chem. Rev.* **1952**, *51*, 119–169. Gordon, J. E. *The Organic Chemistry of Electrolytic Solutions*; Wiley: New York, 1975. Dandliker, W. B.; Alonso, R.; de Saussure, V. A.; Kierszenbaum, F.; Levison, S. A. *Biochemistry* **1967**, *6*, 1460–1467. Hatefi, Y.; Hanstein, W. G. *Proc. Natl. Acad. Sci. U.S.A.* **1969**, *62*, 1129–1136. Kool, E. T.; Breslow, R. *J. Am. Chem. Soc.* **1988**, *110*, 1596–1597.

(36) Reichardt, C. *Solvent and Solvent Effects in Organic Chemistry*, 2nd ed.; VCH: Weinheim, Germany, 1988; pp 35–38.

Table III. Hydrogen Bond Distances and Angles for the Structure Shown in Figure 9[a]

D–H···A	D···A	H···A	D–H···A
N9–H9···O2	2.843(5)	1.945(5)	175.4(4)
N14–H14···O1	2.769(5)	2.052(5)	135.8(4)
N15–H15···O1W	3.012(4)	2.326(4)	132.9(4)
N17–H17···C11	3.168(4)	2.309(4)	159.7(5)
O1W–HWA···C11	3.212(5)	2.208(5)	164.0(4)
O1W–HWB···O2	2.881(5)	1.790(5)	153.3(4)

[a] The hydrogen atom positions were calculated, and the esd's for the parameters involving them are underestimated.

The chloride forms the second ion pair in the ground state that is postulated to be the driving force for increased binding of the dianionic transition state and the phosphorane intermediate. Since the catalysis strategy resides in complexing both guanidiniums to one phosphodiester substrate, the incorporation of another anion into the complex is a complication to catalysis that must be continually monitored.

Structural Studies. The host–guest complexes are less soluble in water than in DMSO, such that in 30% water, the *meso* and *d,l* forms of **3** or **4** and dibenzyl phosphate precipitate from solution, and are quite insoluble in 50% water. X-ray data revealed a monoclinic crystal of space group $P2_1/c$ with $a = 18.010(8)$, $b = 10.708(3)$, and $c = 19.989(7)$ Å, $\beta = 104.83(3)°$, $R = 0.0664$, and a goodness-of-fit being 1.597. The crystal structure of *meso*-**4** and dibenzyl phosphate shows the phosphate bound by two hydrogens of one guanidinium moiety, while a chloride ion is bound to the other guanidinium (Figure 9). The chloride is required in the lattice for charge neutrality. A water molecule bridges the phosphate to the chloride. This structure is likely to exist in the solution state and explains the increased 1:1 binding with the chloride salts relative to tetraphenylborate (Table I) and the increased K_1s with increasing concentrations of NaCl and KCl (Figure 8). Table III shows the hydrogen bond angles and distances within the host–guest complex. The incorporation of the chloride and the water in the crystal structure leads to a widening of the cavity spreading apart the aminoimidazoline moieties. This forces a binding arrangement between the phosphodiester and one of the aminoimidazolines which is nonoptimal. The hydrogen bonds between these groups have heteroatom to heteroatom distances between 2.85 and 2.77 Å, but the N14–H14–O1 bond is severely bent with a N–H–O angle of only 136°. The hydrogen bonding between the water and the aminoimidazoline is also nonoptimal with a heteroatom distance of 3.012(4) Å and a bond angle of 133°. The hydrogen-bond donations from the water to the chloride and the phosphodiester are both near 160°.

To avoid the requirement of two counterions in the crystal lattice of **3** or **4** with dibenzyl phosphate, crystals were grown of a complex between *meso*-**4** and a dianionic phosphomonoester, phenyl phosphate (Figure 10). The X-ray data revealed a monoclinic $P2_1/c$ space group with $a = 10.578(5)$, $b = 8.838(4)$, and $c = 32.07(2)$ Å, $\beta = 96.11(4)°$, $R = 0.0579$, and a goodness-of-fit being 1.343. The crystal structure of *meso*-**4** with phenyl phosphate shows the binding expected for a phosphoester, with two-point bonding from each guanidinium moiety to the guest, as is found in SNase and simple phosphate–guanidinium salts (Figure 1). All the heteroatom–heteroatom hydrogen bond distances between the host and the guest are less than 2.9 Å (Table IV). The hydrogen bond angles are also near optimal, being at the most only 11° from 180°. Thus, the spacers used in **3** and **4** position the aminoimidazoline groups complementary to a tetrahedral phosphoester.

The structure between *meso*-**4** and phenyl phosphate is particularly important for the studies of phosphodiester hydrolysis, not only because it demonstrates host–guest complementarity and the predicted four hydrogen bonds but also because the phenyl phosphate may serve as a suitable model for the dianionic

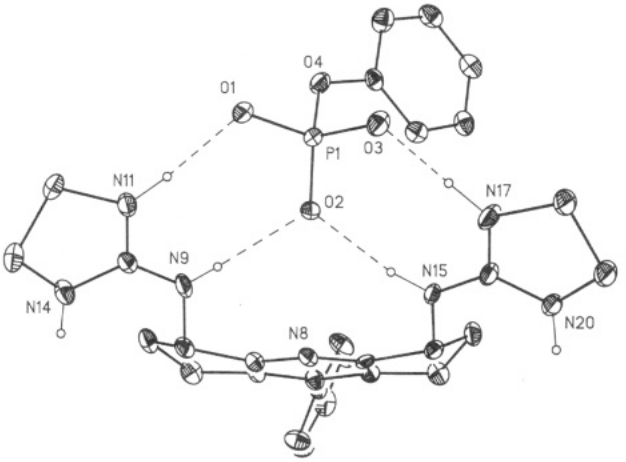

Figure 10. X-ray crystal structure of *meso*-**4** and phenyl phosphate.

Table IV. Hydrogen Bond Distances and Angles for the Structure Shown in Figure 10[a]

D–H···A	D···A	H···A	D–H···A
N9–H9···O2	2.868(6)	2.11(5)	178(5)
N11–H11···O1	2.751(6)	1.84(5)	172(4)
N15–H15···O2	2.840(6)	1.95(5)	169(4)
N17–H17···O3	2.658(7)	1.69(6)	176(5)

[a] The hydrogen atoms were found and refined.

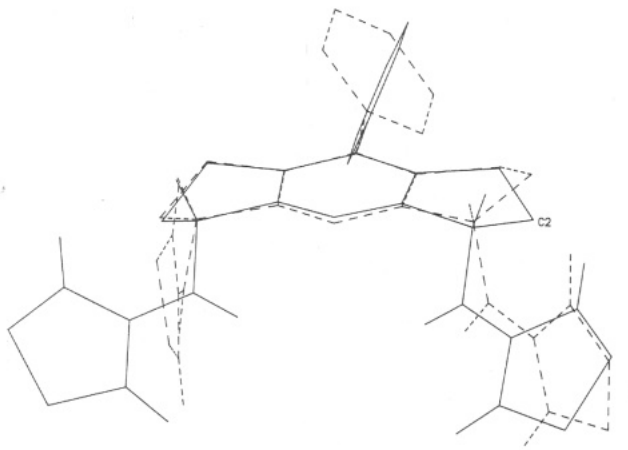

Figure 11. Superposition of *meso*-**4** from the crystal structure with bound chloride and dibenzyl phosphate (– – –) and phenyl phosphate (———), revealing the different puckering modes and bond rotations.

intermediate and the transition state for phosphodiester hydrolysis. Unfortunately, we have not yet measured complexation constants for phosphomonoesters to **3** and **4** due to immediate precipitation upon mixing host and guest in a variety of solvent systems.

The structure of *meso*-**4** with a bound chloride and phosphodiester demonstrates that the receptors possess enough flexibility to bind two separate counterions. The cavities of both **3** and **4** can widen via puckering modes of the cyclohexeno and cyclopenteno rings. Another degree of freedom involves rotation along the aminoimidazoline bond to the spacers. The widening of the cavity with *meso*-**4** to accommodate two anions not only requires a different puckering within the cyclopenteno rings than that used in binding phenyl phosphate but in addition requires that the bond between the spacer and the aminoimidazoline rotate. Both these adjustments within the receptor are shown by the crystal structure superposition given in Figure 11. As discussed above, the tetraphenylborate–*meso* forms of **3** and **4** better accommodate the phosphodiester guest than the *d,l* forms because the guanidinium groups are already preorganized on the same face of the spacer. Conversely, the dichloride *d,l* form of **3** is the better phosphodiester host relative to the *meso* form since a binding

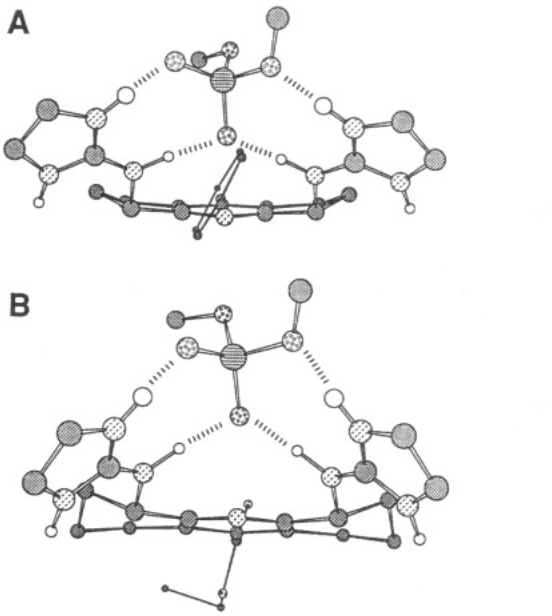

Figure 12. Molecular mechanics-derived host–guest structures: (A) *meso*-**4** and dimethyl phosphate and (B) *meso*-**3** and dimethyl phosphate.

geometry involving both a phosphate and a chloride requires the cavity to be wider. This mode of complexation is most easily accommodated by the *d,l* form of **3**, since the guanidiniums are already on different faces of the spacer and can more easily accommodate two anions.

X-ray quality crystals of dibenzyl phosphate bound in the *meso* forms of **3** and **4** with a tetraphenylborate counterion were not obtainable. We postulate on the basis of molecular mechanics calculations,[37] however, that the binding mode found for phenyl phosphate and *meso*-**4** (Figure 10) represents the most probable structure for *meso*-**3** and *meso*-**4** with dibenzyl phosphate. The calculated structures are shown in Figure 12. The puckering in the cyclopenteno rings of **4** of these molecular mechanics-derived structures is the same as that found in the crystal structure with phenyl phosphate, and the hydrogen bond lengths vary by less than one tenth of an angstrom between the calculated and experimental structures. No crystal data are available for *meso*-**3** as a comparison, but the molecular mechanics again predicts four hydrogen bonds near linearity with all heteroatom distances less than 3.0 Å.

Conclusion

A modular approach to the synthesis of preorganized bis(guanidinium) receptors that complement a phosphodiester has been demonstrated. The syntheses allow for facile manipulation of the cavity size and flexibility and will allow for the future incorporation of RNA recognition units, general bases, and metal-binding sites. Both 1:1 and 2:1 binding of phosphodiesters to these bis(alkylguanidinium) hosts in highly competitive hydrogen-bonding solvents have also been demonstrated. In agreement with predictions from the active site of SNase[14] and simple guanidinium–phosphate salts,[15,16] both guanidiniums in the receptors form two hydrogen bonds to a single bound phosphoester, as supported by the crystal structure of a phosphomonoester, molecular mechanics calculations, and comparison to the binding constants of a simple monoguanidinium receptor. The tetraphenylborate salts of the bis(guanidinium) hosts show stronger binding for the *meso* forms than for the *d,l* forms due to the preorganization of the guanidinium groups on the same face of the relatively rigid spacers. For the chloride salts, *d,l*-**3** binds more strongly than *meso*-**3** due to a special ion effect through a bridging chloride

(37) Still, C. MACROMODEL version 2.5. Columbia University, Amber Force Field.

anion. In addition, the puckering modes within the cyclohexeno and cyclopenteno rings, along with possible bond rotations between the aminoimidazoline groups and the spacers, allow the receptors to open or close and thus accommodate either one or two anionic guests.

meso-**3** has been shown to enhance the imidazole-catalyzed cleavage of mRNA at micromolar concentrations.[10] The current postulate is that catalysis derives from increased binding in the transition-state–receptor complex due to the formation of an additional ion pair that is absent in the substrate–receptor complex. Our current efforts are focused on increasing the rate enhancement and deciphering the details of the mechanism behind the energetic stabilization that bis(guanidinium) receptors impart to phosphodiester hydrolysis.

Experimental Section

General Information. ^{1}H and ^{13}C NMR spectra were obtained in $CDCl_3$, CD_3CN, DMSO-d_6, or D_2O used as purchased without further purification. Spectra were recorded on a General Electric QE-300 (300 MHz) or a Bruker AC-250 (250 MHz) spectrometer. Melting points were measured on a Thomas Hoover capillary melting-point apparatus. Data were not corrected. Elemental analyses were performed by Galbraith Laboratories and Atlantic Laboratories. Low-resolution and high-resolution mass spectra were measured with Finnigan TSQ70 and VG Analytical ZAB2-E instruments, respectively.

All ^{31}P NMR binding studies were performed on a Nicolet NT-360 (146 MHz) spectrometer, and all ^{1}H NMR binding studies were carried out with a General Electric QE-300 (300 MHz) or a Bruker AC-250 (250 MHz) spectrometer. An internal capillary tube was used in some ^{31}P NMR binding studies, which contained triphenylphosphine as a reference (δ = –6.00 ppm). Other studies were referenced to phosphoric acid in D_2O. Syringes and other glassware were dried under vacuum. Exact guest concentrations were determined by UV spectra (Beckman DU-70 UV–vis spectrophotometer).

Solvents and reagents were of reagent grade quality, purchased from Aldrich, and used without further purification except for DME. DME was purified by distillation from sodium–benzophenone ketyl. Preparative flash chromatography was performed on Scientific Adsorbants Incorporated Silica Gel 40 μm. Analytical TLC was performed on precoated Silica Gel 60 F-254 plates.

Syntheses. Ethyl 2,2-Bis(2′-oxocyclohexyl)acetate (7). To a reaction mixture of 7.6 g (75 mmol) of ethyl glyoxylate in 25 mL of benzene was added 18.9 g (130 mmol) of 1-pyrrolidinylcyclohexene, and the reaction was warmed to reflux for 16 h. Then, 35 mL of water was added and the reaction allowed to reflux for 6 h. The solvent was evaporated, and the residue was extracted three times with 25 mL of ether. The extract was dried over $MgSO_4$ and evaporated to dryness on a rotary evaporator. The residue was flashed through a silica gel column with 1:1 ethyl acetate/hexane to give an orange oil which was ready to proceed to the next step. Crude yield: 9.4 g, 55%. Further purification can be achieved by crystallization from the same solvent system to give white crystals. Mp: 158.5–159.5 °C. ^{1}H NMR (300 MHz, $CDCl_3$): δ 4.13 (q, OCH_2CH_3, 2 H), 2.92 (dd, EtO_2CCH, 1 H), 2.63 (s, O=CCH, 1 H), 2.50 (t, O=CCH, 1 H), 2.21–1.30 (m, $CH_2CH_2CH_2CH_2$, 16 H), 1.26 (t, OCH_2CH_3, 3H). ^{13}C [^{1}H] NMR (75 MHz, $CDCl_3$): δ 206.4, 172.9, 60.9, 60.1, 50.4, 48.9, 41.7, 37.0, 31.9, 29.9, 26.8, 26.2, 21.3, 20.1, 14.7. MS-CI: m/z 281 (M^+ + H), 263. Anal. Calcd for $C_{16}H_{24}O_4$: C, 68.43; H, 8.63. Found: C, 67.73; H, 8.64.

1,2,3,4,5,6,7,8-Octahydro-9-acridinecarboxylic Acid Ethyl Ester (8). Compound **7** (6.5 g, 23.3 mmol) and 3.2 g (41.5 mmol) of ammonium acetate were refluxed with 20 mL of glacial acetic acid for 3 h. Water (200 mL) was added, and the mixture was extracted with CH_2Cl_2 (10 mL × 3). The combined dichloromethane layer was washed with 5% $NaHCO_3$ and evaporated under reduced pressure. A ^{1}H NMR spectrum showed the cyclized product which can be purified by silica gel chromatography with 1:2 ethyl acetate/hexane eluent. Yield: 3.6 g, 60%. Mp: 88.5–89.0 °C. ^{1}H NMR (300 MHz, $CDCl_3$): δ 4.32 (q, OCH_2CH_3, 2 H), 2.80 (t, $CCCH_2$, 4 H), 2.60 (t, $NCCH_2$, 4 H), 1.75 (m, CCH_2CH_2, 8 H), 1.30 (t, OCH_2CH_3, 3 H). ^{13}C [^{1}H] NMR (75 MHz, $CDCl_3$): δ 168.0, 154.7, 141.5, 125.0, 61.2, 32.6, 25.7, 22.9, 22.6, 14.2. HRMS-CI: m/z calcd 259.1572 ($C_{16}H_{21}NO_2$), found 259.1559.

4,5-Dibenzylidene-1,2,3,4,5,6,7,8-octahydro-9-acridinecarboxylic Acid Ethyl Ester (9). Compound **8** (2.9 g, 11.3 mmol), 12 g (113 mmol) of benzaldehyde, and 12 mL of acetic anhydride were heated to reflux under N_2 for 10 h. The resulting solution was distilled under vacuum to remove the benzaldehyde and the acetic anhydride. The residue, after distillation, was purified by crystallization from ethyl acetate to give 4.02 g of product, 85% yield. An alternative method was to cool the residue in an ice bath to cause precipitation followed by collecting the precipitate by filtration and crystallization from hexane/EtOAc. Mp: 133.5–134.5 °C. ^{1}H NMR ($CDCl_3$, 300 MHz): δ 8.04 (s, CCH, 2 H), 7.36–7.10 (m, C_6H_5, 10 H), 4.33 (q, J = 7.2 Hz, OCH_2CH_3, 2 H), 2.80 (t, J = 5.4 Hz, $CCCH_2$, 4 H), 2.70 (t, J = 6.0 Hz, $CHCCH_2$, 4 H), 1.75 (t, J = 6.0 Hz, $CH_2CH_2CH_2$, 4 H), 1.32 (t, J = 7.2 Hz, OCH_2CH_3, 3 H). ^{13}C [^{1}H] NMR (75 MHz, $CDCl_3$): δ 168.2, 150.5, 141.6, 138.0, 135.4, 129.6, 128.1, 127.3, 126.8, 126.7, 61.3, 27.7, 22.5, 14.3. MS-EI: m/z 435 (M^+), 362, 343. Anal. Calcd for $C_{30}H_{29}NO_2$: C, 82.76; H, 6.67; N, 3.22. Found: C, 82.13; H, 6.77; N, 3.24.

4,5-Dioxo-1,2,3,4,5,6,7,8-octahydro-9-acridinecarboxylic Acid Ethyl Ester (11). Compound **9** (9.8 g, 23 mmol) was dissolved in 300 mL of CH_2Cl_2 in a three-neck round-bottom flask equipped with a drying tube and a gas inlet. The solution was cooled to –78 °C, and ozone was bubbled through the solution until a blue color persisted. The excess ozone was purged by oxygen. After the blue color disappeared, 5 mL of Me_2S (67 mmol) was added and the mixture allowed to slowly warm to room temperature. The excess dimethyl sulfide and solvent were removed by vacuum. The residue was purified by a silica gel column (1.5 × 7 in.^{2}) with pure EtOAc. The third fraction (R_f = 0.15) was identified as the product. Yield: 3.2 g, 48%. Mp: 164–165 °C. ^{1}H NMR (300 MHz, $CDCl_3$): δ 4.46 (q, J = 7.2 Hz, OCH_2CH_3, 2 H), 2.97 (t, CCH_2, 4 H), 2.80 (t, O=CCH_2, 4 H), 2.15 (m, $CH_2CH_2CH_2$, 4 H), 1.42 (t, OCH_2CH_3, 3 H). ^{13}C [^{1}H] NMR (75 MHz, $CDCl_3$): δ 193.9, 165.8, 147.7, 142.6, 138.9, 62.2, 39.2, 26.8, 21.7, 14.1. MS-EI: m/z 287 (M^+), 230, 122, 105. Anal. Calcd for $C_{16}H_{17}NO_4$: C, 66.9; H, 5.92; N, 4.88. Found: C, 65.46; H, 5.78; N, 4.65.

4,5-Diamino-1,2,3,4,5,6,7,8-octahydro-9-acridinecarboxylic Acid Ethyl Ester (5). A flame-dried 500-mL round-bottom flask was charged with 51.4 g (667 mmol, 21.5 equiv) of ammonium acetate (dried for 1 day under vacuum), 2.89 g (43.79 mmol, 1.4 equiv) of sodium cyanoborohydride, about 50 molecular sieves, 8.90 g (31.02 mmol) of diketone **11**, and 250 mL of absolute ethanol. The inhomogeneous reaction mixture was stirred under nitrogen at room temperature for 93 h and then evaporated. The black oily residue was extracted with 100 mL of dichloromethane and 100 mL of ammonium hydroxide (pH ≃ 12). Sodium chloride was added (~1.0 M) to the aqueous layer, and the water was extracted with 100 mL of dichloromethane three times. All organic portions were combined, dried with magnesium sulfate, and evaporated. Preparative silica gel chromatography with 90:10 dichloromethane/ammonia-saturated methanol yielded 7.32 g (81.7%) of a cream solid. ^{1}H NMR (300 MHz, $CDCl_3$): δ 4.4 (q, CH_2CH_3, 2 H), 3.95 (t, CH, 2 H), 2.7 (m, $PhCH_2$, 4 H), 1.7–2.3 (m, CH_2CH_2, NH_2, 8 H + 4 H), 1.4 (t, CH_2CH_3, 3H). MS: m/z 290 (MW + 1). The full characterization was performed after isomer separation; see below.

4,5-Bis[(1,1-dimethylethoxy)carbonyl]amino]-1,2,3,4,5,6,7,8-octahydro-9-acridinecarboxylic Acid Ethyl Ester (14). A 250-mL round-bottom flask was charged with 7.32 g (25.35 mmol) of diamine **5**, 17.23 g (76.61 mmol, 3.02 equiv) of di-*tert*-butyl dicarbonate, and 150 mL of chloroform. The solution was stirred at room temperature for 21 h. After evaporation, the residue was flashed through a silica gel column with 90:10 dichloromethane/ethyl acetate. Fractions at R_f 0.55–0.40 and R_f 0.35–0.20 were collected separately. Evaporation of both fractions gave colorless solids. Yield: 8.16 g (65.9%); *d,l* isomer, 4.33 g (1st fraction); *meso* isomer, 3.83 g (2nd fraction). ***d,l* isomer**: mp 48–54 °C. ^{1}H NMR (300 MHz, $CDCl_3$): δ 5.57 (br, NH, 2 H), 4.58 (m, CH, 2 H), 4.39 (q, CH_2CH_3, 2 H), 2.68 (m, $PhCH_2$, 4 H), 1.62, 1.89, 2.48 (br, CH_2CH_2, 8 H), 1.49 (s, tBu, 18 H), 1.25 (t, CH_2CH_3, 3 H). ^{13}C [^{1}H] NMR (75 $CDCl_3$ MHz): δ 167.61, 156.16, 153.22, 141.89, 127.12, 79.22, 61.61, 51.87, 29.58, 28.47, 25.33, 19.64, 14.21. MS: m/z 490 (MW + 1). HRMS (CI + mode): m/z calcd 489.2838, found 489.2829. Anal. Calcd for $C_{26}H_{39}N_3O_6$: C, 63.78; H, 8.03; N, 8.58. Found: C, 63.46; H, 8.10; N, 8.67. ***meso* isomer**: mp 129–130 °C. ^{1}H NMR (300 MHz, $CDCl_3$: δ 5.53 (br, NH, 2 H), 4.61 (m, CH, 2 H), 4.40 (q, CH_2CH_3, 2 H), 2.70 (m, $PhCH_2$, 4 H), 1.5–2.5, 1.88 (br, CH_2CH_2, 8 H), 1.48 (s, tBu, 9 H), 1.38 (t, CH_2CH_3, 3 H). ^{13}C [^{1}H] NMR (75 MHz, $CDCl_3$): δ 167.52, 155.96, 153.28, 124.02, 127.22, 79.30, 61.63, 51.63, 29.45, 25.31, 19.53, 14.21. MS-FAB: m/z 490 (MW + 1). HRMS (CI + mode): m/z calcd 489.2838, found 489.2833. Anal. Calcd for $C_{26}H_{39}N_3O_6$: C, 63.78; H, 8.03; N, 8.58. Found: C, 62.33; H, 8.01; N, 8.40.

***meso*- and *d,l*-4,5-Diamino-1,2,3,4,5,6,7,8-octahydro-9-acridinecarboxylic Acid Ethyl Esters 5.** A 250-mL round-bottom flask was charged

with 7.10 g (14.54 mmol) of **14** dissolved in 60 mL of trifluoroacetic acid and 20 mL of water. The solution was stirred at room temperature for 3.5 h and evaporated under vacuum. To the residue was added ammonium hydroxide solution (pH 12 with 1 M NaCl), and the product was extracted with 100 mL of dichloromethane. The aqueous layer was washed with 100 mL of dichloromethane three times. All dichloromethane layers were combined, dried with magnesium sulfate, and evaporated. A white solid was obtained, which showed a single spot on the TLC plate with 90:10 dichloromethane/ammonia-saturated methanol, $R_f = 0.2$. Yield: 3.80 g (90.5%). ***d,l* isomer**: mp 93–94.5 °C. ^{1}H NMR (300 MHz, $CDCl_3$): δ 4.36 (m, CH_2CH_3, 2 H), 3.94 (m, CH, 2 H), 2.65 (m, $PhCH_2$, 4 H), 2.00 (s, NH_2, 4 H), 1.6–2.3 (m, CH_2CH_2, 8 H), 1.36 (t, CH_2CH_3, 3 H). ^{1}H NMR (500 MHz, $CDCl_3$): δ 4.32, 4.33, 4.34, 4.35, 4.36, 4.37, 4.38, 4.39. ^{13}C [^{1}H] NMR (75 MHz, $CDCl_3$): δ 168.16, 157.46, 141.20, 125.27, 61.35, 51.58, 31.75, 26.16, 19.98, 14.25. MS-CI: *m/z* 290 (MW + 1). HRMS (CI + mode): *m/z* calcd for $C_{16}H_{24}N_3O_2$ (product + H^+) 290.1868, found 290.1863. ***meso* isomer**: yield 99.8%; mp 73–75 °C. ^{1}H NMR (300 MHz, $CDCl_3$): δ 4.35 (q, CH_2CH_3, 2 H), 3.93 (m, CH, 2 H), 2.67 (m, $PhCH_2$, 4 H), 2.19 (s, NH, 4 H), 1.6–2.1 (m, CH_2CH_2, 8 H), 1.36 (t, CH_2CH_3, 3 H). ^{1}H NMR (500 MHz, $CDCl_3$): δ 4.33, 4.34, 4.36, 4.37. ^{13}C [^{1}H] NMR (75 MHz, $CDCl_3$): δ 168.06, 157.24, 141.30, 125.39, 61.37, 51.54, 31.61, 26.05, 19.87, 14.22. MS-CI: *m/z* 290 (MW + 1). HRMS (CI + mode): *m/z* calcd for $C_{16}H_{24}N_3O_2$ (product + H^+) 290.1868, found 290.1871.

[[(1,1-Dimethylethoxy)carbonyl]amino]ethylIsothiocyanate (16). Di-*tert*-butyl dicarbonate 17.98 g (79.91 mmol) was dissolved in 200 mL of chloroform and the solution added to a 30.0 mL (449 mmol, 5.62 equiv) solution of ethylenediamine dropwise for 2.5 h. The reaction mixture was stirred at room temperature for 19 h and then evaporated. The oily residue was extracted with 100 mL of Na_2CO_3 and 100 mL of dichloromethane. The aqueous layer was washed with 100 mL of dichloromethane. All dichloromethane layers were combined, dried with magnesium sulfate, and evaporated. The resulting oil was passed through a silica gel column with 90:10 dichloromethane/ammonia-saturated methanol eluent. The fraction at R_f 0.3–0.2 was collected. The product was a colorless oil. Yield: 10.72 g (83.9%). ^{1}H NMR (300 MHz, $CDCl_3$): δ 4.89 (br, NH, 1 H), 3.18 (q, CH_2CH_2NH, 2 H), 2.80 (t, CH_2CH_2NH, 2 H), 1.60 (br, NH, 2 H), 1.44 (s, tBu, 9 H). ^{13}C [^{1}H] NMR (75 MHz, $CDCl_3$): δ 156.21, 79.26, 43.31, 41.83, 28.41. MS: *m/z* 161 (M + 1). A round-bottom flask was charged with 13.17 g (63.22 mmol, 1.0 equiv) of 1,3-dicyclohexylcarbodiimide, 26.0 mL (432 mmol, 6.82 equiv) of carbon disulfide, and 40 mL of THF and cooled to –7 to –10 °C with an NH_4Cl/ice (50 g/200 g) bath. The above oil (10.1 g, 63.2 mmol) was dissolved in 30 mL of dried THF and added dropwise over 30 min to the DCC solution at –7 to –10 °C. The reaction mixture was allowed to warm up to room temperature naturally and stirred at room temperature for 21 h. After evaporation, 400 mL of diethyl ether was added to the residue and a white insoluble solid (dicyclohexylthiourea) was removed by filtration. The filtrate was evaporated and passed through a silica gel column with 80:20 hexanes/ethyl acetate. The fraction at R_f 0.4–0.3 was collected. The product was a white fine solid. Mp: 63–64 °C. Yield: 11.89 g (93.2%). ^{1}H NMR (300 MHz, $CDCl_3$): δ 1.44 (s, tBu, 9 H), 3.37 (q, CH_2CH_2NH, 2 H), 3.63 (t, CH_2CH_2NH, 2 H), 4.90 (br, NH, 1 H). ^{13}C [^{1}H] NMR (75 MHz, $CDCl_3$): δ 155.54, 132.34, 80.13, 45.43, 40.57, 28.31. MS (CI +): *m/z* 203 (MW + 1). HRMS (EI + mode): *m/z* calcd for $C_8H_{14}N_2O_2S$ 202.0776, found 202.0761.

***meso*- and *d,l*-4,5-Bis[[[[2-[[(1,1-dimethylethoxy)carbonyl]amino]-ethyl]amino]thioxomethyl]amino]-1,2,3,4,5,6,7,8-octahydro-9-acridinecarboxylic Acid Ethyl Esters 17.** A round-bottom flask was charged with 3.80 g (13.1 mmol) of **5**, 6.7032 g (33.18 mmol, 2.52 equiv) of **16**, and 250 mL of absolute ethanol. The reaction mixture was stirred at room temperature for 23 h during which time a precipitate formed. After evaporation, the residue was passed through a silica gel column eluted with 98:2 dichloromethane/methanol. The fraction at R_f 0.1 was collected. Yield: 7.23 g (78.7%). ***d,l* isomer**: mp 112.5–122.5 °C. ^{1}H NMR (300 MHz, DMSO-d_6): δ 7.80 (m, NH, 2 H), 7.41 (br, NH, 2 H), 6.83 (m, NH, 2 H), 5.17 (br, CH, 2 H), 4.36 (q, CH_2CH_3, 2 H), 3.42 (br, $NHCH_2CH_2NH$, 4 H), 3.06 (m, $NHCH_2CH_2NH$, 4 H), 2.62 (br, $PhCH_2$, 4 H), 1.74, 1.96 (br, CH_2CH_2, 8 H), 1.35 (s, tBu, 18 H), 1.29 (t, CH_2CH_3, 3 H). ^{13}C [^{1}H] NMR (75 MHz, DMSO-d_6): δ 181.74, 166.91, 155.71, 153.35, 141.58, 127.25, 77.69, 61.48, 54.85, 53.50, 43.34, 28.49, 28.18, 25.09, 17.93, 13.96, MS-CI: *m/z* 694 (MW + 1). HRMS (CI + mode): *m/z* calcd for $C_{32}H_{52}N_7O_6S_2$ (M + H^+) 694.3420, found 694.3410. Anal. Calcd for $C_{32}H_{51}N_7O_6S_2$: C, 55.39; H, 7.41; N, 14.13. Found: C, 54.81; H, 7.40; N, 14.00. ***meso* isomer**: yield 85.7%; mp 113–116.5 °C. ^{1}H NMR (300 MHz, DMSO-d_6): δ 7.66 (br, NH, 4 H), 6.83 (m, NH, 2 H), 5.11 (br, NH, 2 H), 4.35 (q, CH_2CH_3, 2 H), 3.39 (br, $NHCH_2CH_2NH$, 4 H), 3.08 (m, $NHCH_2CH_2NH$, 4 H), 2.61 (m, $PhCH_2$, 4 H), 1.7–2.2 (br, CH_2CH_2, 8 H), 1.33 (s, tBu, 18 H), 1.32 (t, CH_2CH_3, 3 H). ^{13}C [^{1}H] NMR (75 MHz, DMSO-d_6): δ 181.96, 166.81, 155.73, 153.25, 141.69, 127.05, 77.70, 61.51, 54.85, 53.61, 43.70, 28.71, 28.16, 24.86, 18.47, 13.96. MS (CI –): *m/z* 693 (MW). HRMS: *m/z* calcd for $C_{32}H_{51}N_7O_6S_2$ 693.3342, found 693.3330. Anal. Calcd for $C_{32}H_{51}N_7O_6S_2$: C, 55.39; H, 7.41; N, 14.13. Found: C, 54.55; H, 7.39; N, 13.87.

***meso*- and *d,l*-*N,N'*-Bis(4,5-dihydro-1*H*-imidazol-2-yl)-1,2,3,4,5,6,7,8-octahydro-9-acridinecarboxylic Acid Ethyl Esters 3.** A round-bottom flask was charged with 7.01 g (10.12 mmol) of **17**, 100 mL (1.34 mol, 132 equiv) of bromoethane, and 100 mL of absolute ethanol. The reaction mixture was allowed to reflux gently (oil bath, 50–60 °C) for 18 h. After reaction, the solution was evaporated and dried under vacuum. The product was an oily solid and used in the next step without purification. The oil (9.21 g, 10.12 mmol) was dissolved in 60.0 mL (779 mmol, 77.0 equiv) of trifluoroacetic acid and 20 mL of water, and the solution was stirred at room temperature for 2.5 h. The solvent was evaporated under vacuum to yield a brown solid which was used in the next step without further purification. Sodium (1.47 g, 64.08 mmol, 6.33 equiv) was dissolved in 500 mL of absolute ethanol. The brown solid (10.17 g, 10.12 mmol) was dissolved in 100 mL of absolute ethanol and added dropwise to the sodium ethoxide solution at room temperature over 30 min. The reaction mixture was stirred for an additional 20 min. After evaporation, the residue was passed through a silica gel column with 85:15 dichloromethane/methanol as eluent. The product was a slightly hygroscopic solid. Yield: 4.07 g (94.7%) from **9**. ***d,l* isomer.** ^{1}H NMR (300 MHz, DMSO-d_6): δ 7.5–9.0 (br, NH, 4 H), 4.65 (m, CH, 2 H), 4.37 (q, CH_2CH_3, 2 H), 3.63 (s, $NHCH_2CH_2NH$, 8 H), 2.65 (m, $PhCH_2$, 4 H), 1.7–2.2 (m, CH_2CH_2, 8 H), 1.30 (t, CH_2CH_3, 3 H). ^{13}C [^{1}H] NMR (75 MHz, DMSO-d_6): δ 166.48, 159.09, 151.92, 141.80, 127.75, 61.70, 52.68, 42.50, 28.76, 24.79, 18.18, 13.92, MS (CI –): *m/z* 425.5 (MW). HRMS (CI – mode) calcd for $C_{22}H_{31}N_7O_2$ 425.2539, found 425.2539. ***meso* isomer**: yield 85.3% (from **9**). ^{1}H NMR (300 MHz, DMSO-d_6): δ 7.8–9.0 (br, NH, 4 H), 4.65 (m, CH, 2 H), 4.36 (q, CH_2CH_3, 2 H), 3.62 (s, $NHCH_2CH_2NH$, 8 H), 2.64 (m, $PhCH_2$, 4 H), 1.7–2.2 (m, CH_2CH_2, 8 H), 1.29 (t, CH_2CH_3, 3 H). ^{13}C [^{1}H] NMR (75 MHz, DMSO-d_6): δ 166.68, 159.65, 152.29, 142.06, 127.74, 61.91, 52.88, 42.76, 28.87, 24.93, 18.63, 14.13. HRMS (CI – mode): *m/z* calcd for $C_{22}H_{31}N_7O_2$ 425.2539, found 425.2513.

***meso*- and *d,l*-*N,N'*-Bis(4,5-dihydro-1*H*-imidazol-2-yl)-1,2,3,4,5,6,7,8-octahydro-9-acridinecarboxylic Acid Ethyl Ester Dihydropicrates 3.** Picric acid (0.27 g, 1.07 mmol, 4.1 equiv) was dissolved in 50 mL of hot water, and to this solution was added 0.1125 g (0.2647 mmol) of *meso*-**3** or *d,l*-**3** in 7 mL of water. After the solution was cooled to room temperature, the yellow precipitates were collected by filtration and washed with water. The precipitates were purified by crystallization from acetonitrile and ethyl acetate. ***d,l* isomer**: mp 218–219 °C. ^{1}H NMR (300 MHz, DMSO-d_6): δ 8.59 (d, NH, 2 H), 8.57 (s, PicH, 4 H), 7.4–9.0 (br, NH, 4 H), 4.63 (m, CH, 2 H), 4.36 (q, CH_2CH_3, 2 H), 3.63 (s, $NH(CH_2)_2NH$, 8 H), 2.64 (m, $PhCH_2$, 4 H), 1.7–2.2 (br, CH_2CH_2, 8 H), 1.29 (t, CH_2CH_3, 3 H). ^{13}C [^{1}H] (72.5 MHz, DMSO): δ 166.46, 160.77, 159.08, 151.97, 141.88, 141.79, 127.86, 125.21, 124.34, 61.71, 52.68, 42.57, 28.73, 24.82, 18.13, 13.91. Anal. Calcd for $C_{34}H_{37}N_{13}O_{16}\cdot H_2O$: C, 45.28; H, 4.35; N, 20.18. Found: C, 45.53; H, 4.13; N, 20.38. ***meso*-isomer**: mp 247.5–248.5 °C dec. ^{1}H NMR (300 MHz, DMSO-d_6): δ 8.57 (s, NH, 4 H), 8.51 (d, PicH, 2 H), 7.5–9.0 (br, NH, 4 H), 4.62 (m, CH, 2 H), 4.36 (q, CH_2CH_3, 2 H), 3.62 (s, $NH(CH_2)_2NH$, 8 H), 2.64 (m, $PhCH_2$, 4 H), 1.7–2.2 (br, CH_2CH_2, 8 H), 1.29 (t, CH_2CH_3, 3 H). ^{13}C [^{1}H] (72.5 MHz, DMSO-d_6): δ 166.50, 159.44, 152.09, 141.93, 141.84, 127.63, 125.20, 61.77, 56.04, 52.67, 42.63, 28.63, 24.76, 18.53, 18.42, 13.96. Anal. Calcd for $C_{34}H_{37}N_{13}O_{16}\cdot 2H_2O$: C, 45.28; H, 4.35; N, 20.18. Found: C, 45.81; H, 4.15; N, 20.36.

***meso*- and *d,l*-*N,N'*-Bis(4,5-dihydro-1*H*-imidazol-2-yl)-1,2,3,4,5,6,7,8-octahydro-9-acridinecarboxylic Acid Ethyl Ester Dihydrochlorides 3.** The picrate crystals were dissolved in a minimum amount of THF/H_2O with 1–2 drops of concentrated aqueous HCl and then eluted on Amberlite IRA-400 (Cl^-) resin. The resin was washed with water, and the effluent was collected fractionally. The fractions were spotted on a silica gel plate in the presence of iodine vapor. Iodine-active fractions were collected and lyophilized twice. A fine pale yellow solid was obtained. ***d,l* isomer**: Yield 0.056 g (from free base) 42.8%. ^{1}H NMR (300 MHz, DMSO-d_6): δ 8.81 (d, NH, 2 H), 7.5–9.0 (br, NH, 4 H), 4.72 (t, CH, 2 H), 4.36 (q, CH_2CH_3, 2 H), 3.62 (s, $NHCH_2CH_2NH$, 8 H), 2.64 (m, $PhCH_2$, 4 H),

1.7–2.2 (m, CH_2CH_2, 8 H), 1.29 (t, CH_2CH_3, 3 H). ^{13}C [^1H] NMR (75 MHz, DMSO-d_6): δ 166.49, 159.24, 152.07, 141.71, 127.54, 61.65, 52.69, 42.49, 28.82, 24.77, 18.36, 13.91. Anal. Calcd for $C_{22}H_{33}N_7O_2Cl_2 \cdot 2H_2O$: C, 49.44; H, 6.22; N, 18.34. Found: C, 50.62; H, 6.56; N, 18.23. ***meso* isomer**: yield 45.7% (from free base). ^1H NMR (300 MHz, DMSO-d_6): δ 8.78 (d, NH, 2 H), 7.6–9.0 (br, NH, 4 H), 4.85 (m, CH, 2 H), 4.35 (q, CH_2CH_3, 2 H), 3.63 (s, $NHCH_2CH_2NH$, 8 H), 2.64 (m, $PhCH_2$, 4 H), 1.7–2.3 (m, CH_2CH_2, 8 H), 1.29 (t, CH_2CH_3, 3 H). ^{13}C [^1H] NMR (75 MHz, DMSO-d_6): δ 166.72, 159.87, 152.13, 142.07, 127.52, 53.27, 61.86, 42.70, 29.19, 24.77, 18.99, 14.13. Anal. Calcd for $C_{22}H_{33}N_7O_2Cl_2 \cdot 4H_2O$): C, 46.30; H, 7.17; N, 16.99. Found: C, 46.31; H, 7.24; N, 17.19.

***meso*- and *d,l*-*N,N'*-Bis(4,5-dihydro-1*H*-imidazol-2-yl)-1,2,3,4,5,6,7,8-octahydro-9-acridinecarboxylic Acid Ethyl Ester Dihydrotetraphenylborates 3.** **3** dichloride (112 mg, 0.226 mmol) was dissolved in 20 mL of water, and an aqueous solution of sodium tetraphenylborate (170 mg, 0.497 mmol) was added. The solution was lyophilized and dissolved in acetonitrile. The insoluble NaCl was removed by filtration through Celite and the acetonitrile removed under vacuum. Yield: 249.8 mg, 88%. ***meso* isomer**: mp 117–118 °C. ^1H NMR (250 MHz, CD_3CN): δ 6.83, 6.99, 7.29 (tts, TPB, 40 H), 4.49 (t, CH, 2 H), 4.41 (q, CH_2CH_3, 2 H), 3.59 (s, $NHCH_2NH$, 8 H), 2.73 (m, $PhCH_2$, 4 H), 1.34 (t, CH_2CH_3, 3 H), 1.85, 2.17 (m, CH_2CH_2, 8 H). ^{13}C NMR [^1H] (72.5 MHz, CD_3CN): δ 167.55, 164.5 (q), 161.01, 152.43, 136.64, 129.64, 126.55, 126.50, 122.68, 62.98, 54.44, 43.83, 29.44, 25.79, 19.39, 14.45. Anal. Calcd for $C_{70}H_{73}N_7O_2B_2 \cdot 3H_2O$: C, 75.06; H, 7.10; N, 8.75. Found: C, 76.64; H, 6.94; N, 9.48. ***d,l* isomer**: mp 121.5–122.5 °C. ^1H NMR (250 MHz, $CDCl_3$): δ 6.87, 7.00, 7.26 (ttd, TPB, 40 H), 4.48 (m, CH, 2 H), 4.39 (q, CH_2CH_3, 2 H), 3.59 (s, $NHCH_2CH_2NH$, 8 H), 1.90, 2.08, 2.71 (m, CH_2CH_2, 8 H), 1.34 (t, CH_2CH_3, 3 H). ^{13}C NMR [^1H] (72.5 MHz, $CDCl_3$): δ 170.18, 164.60 (q), 164.52, 160.50, 152.60, 144.17, 136.74, 126.66, 125.45, 62.90, 54.56, 43.93, 29.48, 25.87, 19.50, 14.45. Anal. Calcd for $C_{70}H_{73}N_7O_2B_2 \cdot 2H_2O$: C, 76.29; H, 7.04; N, 8.89. Found: C, 76.64; H, 6.94; N, 9.48.

***N*-(4,5-Dihydro-1*H*-imidazol-2-yl)-cyclohexylamine Hydropicrate, Hydrochloride, and Hydrotetraphenylborate 19.** 2-(Methylthio)-2-imidazoline hydroiodide (1.00 g, 4.10 mmol), 0.262 g (3.85 mmol) of sodium ethoxide, and 3.0 mL (26.23 mmol) of cyclohexylamine were combined in a round-bottom flask. The reaction mixture was heated at 90–100 °C, and equimolar amounts of 2-(methylthio)-2-imidazoline hydroiodide and sodium ethoxide along with a minimum amount of DMF were added portionwise over 27.5 h. The solvent was removed under vacuum, and the resulting orange oily solid was passed through a silica gel column with a 95:5 dichloromethane/ammonia-saturated methanol eluent. The fraction at R_f 0.2–0.1 was collected as the product. Further purification was performed by adding 6.70 g (26.37 mmol, 1.0 equiv) of picric acid in hot water. After the solution was cooled to room temperature, the yellow precipitate was collected by filtration. The yellow precipitate was crystallized from 100 mL of acetonitrile, which gave fine needle crystals. Yield: 4.22 g (40.6%). The monoguanidinium picrate was converted to the chloride by the same procedure as that of diguanidine compounds. Yield: 63.2%. Picrate **19**: mp 220.5–221.5 °C. ^1H NMR (300 MHz, DMSO-d_6): δ 8.57 (s, PicH, 2 H), 8.11 (d, NH, 1 H), 7.3–8.5 (br, NH, 2 H), 3.55 (s, CH_2CH_2, 4 H), 3.24 (m, CH, 1 H), 1.19, 1.55, 1.65, 1.80 (m, $(CH_2)_5$, 10 H). ^{13}C [^1H] NMR (75 MHz, DMSO-d_6): δ 160.79, 158.25, 147.80, 125.15, 124.21, 51.40, 42.34, 32.28, 24.63, 24.16. Anal. Calcd for $C_{15}H_{20}N_6O_7$: C, 45.45; H, 5.09; N, 21.20. Found: C, 45.45; H, 5.02; N, 21.38. **Chloride 19**: mp 186.5–187 °C. ^1H NMR (300 MHz, DMSO-d_6): δ 8.42 (d, PicH, 1 H), 7.3–8.8 (br, NH, 2 H), 3.54 (s, CH_2CH_2, 4 H), 3.33 (m, 1 H), 1.21, 1.50, 1.64, 1.80 (m, $(CH_2)_5$, 10 H). ^{13}C [^1H] NMR (75 MHz, DMSO-d_6): δ 158.36, 51.18, 42.28, 32.25, 24.65, 23.97. Anal. Calcd for $C_9H_{18}N_3Cl$: C, 53.06; H, 8.91; N, 20.62. Found: C, 52.08; H, 8.89; N, 20.05. **Tetraphenylborate Salt 19**: mp 151–152 °C. ^1H NMR (250 MHz, $CDCl_3$): δ 6.92, 7.05, 7.41 (tts, TPB, 20 H), 3.51 (d, NH, 1 H), 2.98 (s, CH, 2 H), 2.41 (s, CH_2CH_2, 4 H), 2.18 (m, CH, 1 H), 0.85, 1.10, 1.49 (m, $(CH_2)_5$, 10 H). Anal. Calcd for $C_{33}H_{38}N_3B$: C, 81.24; H, 7.86; N, 8.62. Found: C, 80.27; H, 7.95; N, 8.66.

3,5-Dibenzylidene-1,2,3,5,6,7-hexahydro-8-phenyldicyclopenta[*b,e*]-pyridine (10). Cyclopentanone (0.25 mol, 18.4 mL), benzaldehyde (0.5 mol, 50.8 mL), and ammonium acetate (0.25 mol, 19.3 g) were dissolved in 250 mL of absolute ethanol in an Erlenmeyer flask and warmed to reflux with stirring for 1 h. During this time, the solution changed from colorless to orange and a yellow-orange precipitate formed. After the solution was cooled on ice, the supernatant was decanted, leaving behind a pasty mass, which was washed with methylene chloride, leaving 8 g of a light yellow powder (15%). Mp: 213–215 °C. ^1H NMR (250 MHz, $CDCl_3$): δ 7.9–7.0 (m, C_6H_5, CCH, 17 H), 3.0 (dt, CH_2CH_2, 8 H). ^{13}C [^1H] NMR (72.5 MHz, $CDCl_3$): δ 160.88, 141.63, 137.97, 136.78, 129.05, 128.57, 128.39, 128.08, 126.67, 121.93, 29.37, 27.68. HRMS: *m/z* calcd for $C_{31}H_{25}N$ 411.1987, found 411.1975.

3,5-Dioxo-1,2,3,5,6,7-hexahydro-8-phenyldicyclopenta[*b,e*]pyridine (12). Compound **10** (0.043 mol, 17.5 g) was dissolved in 1000 mL of methylene chloride in a 2000-mL three-necked round-bottom flask fitted with a drying tube, a gas inlet adapter, and a stopper. The solution was cooled in a dry ice/acetone bath (**10** precipitates with cooling). Ozone was bubbled through the solution via the gas inlet for approximately 20 min. The flask was raised out of the cooling bath until the precipitated **10** was redissolved, about 10 min. The flask was returned to the dry ice/acetone bath for the remainder of the ozonolysis time, another 10–15 min. Completion of reaction was signaled by a color change from yellow to pale blue. The solution was purged with oxygen for about 10 min to remove excess ozone, and 3 equiv of dimethyl sulfide was added to the solution. The mixture was gradually warmed to room temperature and stirred for 12 h. The solvent was removed by rotary evaporation, leaving behind a dark brown oil. Purification was done on a silica gel flash column with 70:30 ethyl acetate/hexane as eluent (R_f = 0.5). Yield: 7.4 g, (66%). Mp: 215–217 °C. ^1H NMR (250 MHz, $CDCl_3$): δ 7.6–7.35 (m, C_6H_5, 5 H); 3.12 (t, CH_2CH_2, 4 H), 2.83 (t, CH_2CH_2, 4 H). ^{13}C [^1H] NMR (72.5 MHz, $CDCl_3$): δ 203.96, 155.81, 150.46, 148.20, 133.42, 129.42, 129.26, 127.85, 35.67, 23.05. HRMS: calcd for $C_{17}H_{14}NO_2$ 264.1024, found 264.1019.

3,5-Bis(hydroxyimino)-1,2,3,5,6,7-hexahydro-8-phenyldicyclopenta-[*b,e*]pyridine (13). Compound **12** (0.019 mol, 5 g) was dissolved in 40 mL of dimethylformamide in a 250-mL round-bottom flask fitted with a reflux condenser. Five equivalents (0.095 mol, 10 g) of sodium carbonate and 4 equiv (0.072 mol, 5 g) of hydroxylamine hydrochloride were added with stirring. The mixture was heated on an oil bath to 80 °C for 3 h, during which time a cream-colored precipitate formed. The mixture was allowed to cool, and dimethyl formamide was removed under vacuum overnight. The precipitate was suspended in cold water, filtered, and washed with cold ethanol and ether. Yield: 4.4 g (79%). Mp: 285 °C dec. ^1H NMR (250 MHz, DMSO-d_6): δ 11.31 (s, NOH, 2 H), 7.48 (m, C_6H_5, 5 H), 2.81 (m, CH_2CH_2, 8 H). ^{13}C [^1H] NMR (72.5 MHz, DMSO-d_6): δ 159.47, 155.75, 143.86, 140.46, 135.36, 128.65, 128.41, 128.13, 24.90, 24.78. HRMS: *m/z* calcd for $C_{17}H_{15}N_3O_2$ 293.1164, found 293.1161.

3,5-Diamino-1,2,3,5,6,7-hexahydro-8-phenyldicyclopenta[*b,e*]pyridine (6). Sodium borohydride (0.112 mol, 4.1 g, 8 equiv) and titanium(IV) tetrachloride (0.056, 6 mL, 4 equiv) were combined in a 1000-mL round-bottom flask in a drybox. The flask was fitted with a rubber septum, removed from the drybox, equipped with a nitrogen balloon, and cooled on an ice bath. Freshly distilled dimethoxyethane (100 mL) was added slowly while the flask was vented with a large bore needle. Compound **13** (0.014 mol, 4 g) (dried over phosphorus pentoxide under vacuum) was added as a powder over 5 min. The reaction mixture changed color over half an hour, from bright green to green-brown. The solution was allowed to warm to room temperature and stirred for 24 h. The mixture was cooled on ice, and water (200 mL) was added slowly to quench the reaction. The solution was basified with aqueous ammonia to pH 13, at which point it became gelatinous and turned dark blue. The aqueous layer was extracted several times with methylene chloride (total 1000 mL). The organic layer was dried over sodium sulfate, filtered, and evaporated to dryness on a rotary evaporator. Yield: 1.7 g (60%). ^1H NMR (250 MHz, $CDCl_3$): δ 7.4–7.2 (m, C_6H_5, 5 H), 4.35 (t, CH_2CH_2CH, 2 H), 3.0–2.0 (m, CH_2CH_2, 8 H). The compound was fully characterized after isomer separation.

***meso*- and *d,l*-3,5-Bis[[(1,1-dimethylethoxy)carbonyl]amino]-1,2,3,5,6,7-hexahydro-8-phenyldicyclopenta[*b,e*]pyridines 15.** Compound **6** (0.011 mol, 3 g) was dissolved in chloroform, and di-*tert*-butyl dicarbonate (0.033 mol, 7.2 g, 3 equiv) was added with stirring over a period of 15 min. The flask was fitted with a septum and a nitrogen balloon and allowed to stir for another 45 min. The solvent was removed on a rotary evaporator. TLC of the reaction mixture in 70:30 hexane/ethyl acetate gave R_f values for the *d,l* and *meso* isomers of 0.38 and 0.23, respectively. Separation of the *d,l* and *meso* isomers was achieved on a flash column with 70:30 hexane/ethyl acetate eluent. The appearance of the *d,l* isomers was observed as a white precipitate forming on the tip of the column. The flow was then reduced to gravity flow until the first fraction was finished and then the flow rate was increased again. Yield of each isomer: 50%, 1 g each. ***meso* isomer**: mp 162–165 °C. ^1H NMR (250 MHz, $CDCl_3$): δ 7.5–7.3 (m, C_6H_5, 5 H), 5.2 (s, NH, 2 H), 4.95 (q, CH_2CHNH, 2 H),

3.5–3.0 (m, CH2C*H*H, 6 H), 1.95 (m, CH*H*, 2 H), 1.48 (s, $COC(CH_3)_3$, 18 H). ^{13}C [^1H] NMR (72.5 MHz, $CDCl_3$): δ 161.99, 155.95, 143.74, 136.49, 134.06, 128.21, 79.45, 56.31, 33.82, 28.44, 26.99. HRMS: *m/z* calcd for $C_{27}H_{35}N_3O_4$ 465.2627, found 465.2634. ***d,l* isomer**: mp 179–182 °C. All the ^1H NMR resonances are the same for the *d,l* isomer as for the *meso* except the peak at 5.2 is shifted to 5.35. ^{13}C [^1H] NMR (72.5 MHz, $CDCl_3$): δ 161.99, 156.09, 143.25, 136.27, 133.75, 128.37, 79.38, 56.47, 34.55, 28.31, 27.31. HRMS: *m/z* calcd for $C_{27}H_{35}N_3O_4$ 465.2627, found 465.2632.

***meso*- and *d,l*-3,5-Diamino-1,2,3,5,6,7-hexahydro-8-phenyldicyclopenta[*b,e*]pyridines 6.** Compound **15** (0.0064 mol, 3 g) was dissolved in a mixture of 10 mL of trifluoroacetic acid and 10 mL of H_2O. The solution was stirred for 4 h and the solvent removed under vacuum. The resulting paste was dissolved in 200 mL of 1 M sodium chloride in aqueous ammonia (pH 13). The amine was extracted from the aqueous layer with four 75-mL fractions of dichloromethane. After the solution was dried over sodium sulfate, the dichloromethane was removed by rotary evaporation. Yield: 1.15 g (68%). ***meso* isomer**: mp 134–139 °C. ^1H NMR (250 MHz, $CDCl_3$): δ 7.43–7.26 (m, C_6H_5, 5 H), 4.37 (t, C*H*, 2 H), 2.85–2.49 (m, $PhCH_2CH_2$, NH_2, 10 H), 1.76 (m, CH_2, 2 H). ^{13}C [^1H] NMR (72.5 MHz, $CDCL_3$): δ 165.82, 143.37, 137.05, 132.72, 128.85, 128.42, 128.24, 127.95, 53.37, 32.41, 26.05. HRMS: *m/z* calcd for $C_{17}H_{19}N_3$ 265.1579, found 265.1569. ***d,l* isomer**: mp 163–165 °C. ^1H NMR ($CDCl_3$): δ 7.4–7.2 (m, C_6H_5, 5 H), 4.37 (t, CH, 2 H), 2.79–2.60 (m, $PhCH_2CH_2$, NH_2, 10 H), 1.68 (m, CH_2, 2 H). ^{13}C [^1H] NMR (72.5 MHz, $CDCl_3$) δ 166.14, 143.02, 136.98, 132.45, 128.34, 127.94, 56.74, 34.91, 27.06. HRMS: *m/z* calcd for $C_{17}H_{19}N_3$ 265.1579, found 265.1570.

***meso*- and *d,l*-3,5-Bis[[[[2-[[(1,1-dimethylethoxy)carbonyl]amino]-ethyl]amino]thioxomethyl]amino]-1,2,3,5,6,7-hexahydro-8-phenyldicyclopenta[*b,e*]pyridines 18.** Compound **16** (0.005 mol, 1.05 g, 2.5 equiv) in 50 mL of absolute ethanol was added dropwise to compound **6** (0.002 mol, 550 mg) dissolved in 25 mL of absolute ethanol. The solution was stirred for 20 h under a positive pressure of nitrogen. TLC in 98:2 methylene chloride/methanol (developed with iodine) revealed the product at an R_f of 0.25. Flash silica gel chromatography in the same eluent gave 2.3 g (67%) for the *d,l* isomer and 3.4 g (quantitative) for the *meso* isomer. ***meso* isomer**: mp 73–75 °C. ^1H NMR (250 MHz, $CDCl_3$): δ 7.7–7.3 (m, C_6H_5, 5 H), 5.3 (br t, CH_2CH_2NH, 2 H), 3.7 (br, $NHCH_2$, 4 H), 3.3 (br, $NHCH_2$, 4 H), 2.75 (br, CH_2CH_2, 4 H), 1.95 (br, CH_2CH_2, 4 H), 1.3 (s, $C(CH_3)_3$, 18 H). ^{13}C [^1H] NMR (72.5 MHz, $CDCl_3$): δ 180.84, 161.36, 150.09, 144.43, 135.82, 134.75, 128.44, 128.33, 128.00, 83.13, 79.38, 59.30, 52.66, 47.57, 45.22, 40.89, 40.43, 32.66, 28.16, 27.88, 27.14, 25.24, 24.58. HRMS: *m/z* calcd for $C_{33}H_{47}N_7O_4S_2$ 669.3131, found 699.3130. ***d,l* isomer**: mp 104–112 °C. ^1H NMR (250 MHz, $CDCl_3$): δ 7.47, 7.24 (m, C_6H_5, 5 H), 5.65 (br s, NH, 2 H), 3.84 (br s, NH, 2 H), 3.4 (br s, NH, 2 H), 2.81 (m, CH_2CH_2), 2.2–1.7 (m, CH_2, 4 H), 1.26 (s, tBu, 18 H). ^{13}C [^1H] NMR (72.5 MHz, $CDCl_3$): δ 183.12, 162.28, 157.19, 144.67, 135.68, 134.68, 128.72, 128.06, 79.68, 77.21, 59.31, 52.84, 40.86, 40.61, 33.61, 32.84, 28.31, 28.24, 28.06, 27.23, 25.40, 24.67. HRMS: *m/z* calcd for $C_{33}H_{47}N_7O_4S_2$ 699.3131, found 699.3120.

***meso*- and *d,l*-*N,N'*-Bis(4,5-dihydro-1*H*-imidazol-2-yl)-1,2,3,5,6,7-hexahydro-8-phenyldicyclopenta[*b,e*]pyridine-3,5-diamines 4.** Compound *meso*-**18** (0.0015 mol, 0.9 g) and compound *d,l*-**18** (0.0025 mol, 1.5 g) were each dissolved in a solution of 10 mL of bromoethane and 10 mL of absolute ethanol. Each flask was fitted with a reflux condenser and a nitrogen ballon, and the mixtures were refluxed for 20 h. A TLC in 90:10 methylene chloride/methanol confirmed formation of the product, with an R_f of 0.72 for the *meso* isomer and 0.61 for the *d,l* isomer. The solvent was removed by rotary evaporation. This product was not isolated. The resulting oils were each dissolved in about 6 mL of trifluoroacetic acid and 3 mL of H_2O and stirred at room temperature for 3–4 h. TLC in 90:10 methylene chloride/methanol saturated with NH_3 showed a product with an R_f of 0.37 for the *d,l* isomer and 0.44 for the *meso* isomer. The TFA was removed under vacuum overnight and the product lyophilized. This product was not isolated but taken directly to the next step. Approximately 100 mg of sodium was dissolved in 10 mL of absolute ethanol. The resulting solid from the previous step was dissolved in 20 mL of absolute ethanol and added dropwise to the sodium ethoxide solution over 2 h. The system was sealed with a balloon and stirred for 24–36 h, and the solvent was removed by rotary evaporation. ***meso* isomer**: yield 522 mg (90%). ^1H NMR (250 MHz, $CDCl_3$): δ 8.89 (br s, NH, 2 H), 8.61 (d, NH, 2 H), 7.96 (br s, NH, 2 H), 7.42, 7.25 (m, C_6H_5, 5 H), 5.11 (q, CH_2CHNH, 2 H), 3.67 (s, $NHCH_2CH_2NH$, 8 H), 2.67, 1.88 (m, CCH_2CH_2CH, 8 H). ^{13}C [^1H] NMR (72.5 MHz, $CDCl_3$): δ 162.72, 162.18, 161.63, 161.88, 160.78, 160.37, 160.22, 144.52, 135.59, 135.75, 128.64, 128.03, 57.72, 45.19, 32.73, 27.08. ***d,l* isomer**: yield 600 mg (62%). ^1H NMR (250 MHz, $CDCl_3$): δ 9.43 (d, NH, 2 H), 9.18 (br s, NH, 2 H), 7.96 (br s, NH, 2 H), 7.43, 7.28 (m, 2 H, 5 H), 4.82 (q, CH_2CHNH, 2 H), 3.66, (s, $NHCH_2CH_2NH$, 8 H), 2.9–2.7, 1.92 (m, CCH_2CH_2CH, 8 H). ^{13}C [^1H] NMR (72.5 MHz, $CDCl_3$) 163.52, 162.96, 162.41, 161.85, 160.87, 160.83, 144.32, 135.99, 134.14, 128.81, 128.72, 128.14, 118.93, 114.27, 57.66, 43.05, 32.17, 27.36.

***meso*- and *d,l*-*N,N'*-Bis(4,5-dihydro-1*H*-imidazol-2-yl)-1,2,3,5,6,7-hexahydro-8-phenyldicyclopenta[*b,e*]pyridine-3,5-diamine Dihydropicrates 4.** Compounds *meso*-**4** and *d,l*-**4** were purified by conversion to picrate salts in the following manner. Each compound (3.62 mmol, 1.4 g) was dissolved in 80 mL of water. Picric acid (8 mmol, 1.82 g, 2.2 equiv) was dissolved in 100 mL of water. The solutions were heated to boiling and then combined, at which time a precipitate formed. The mixture was allowed to stand overnight and then filtered and washed with cold water, ethanol, and ether. The same procedure was used for the *d,l* compound except it was found that the solutions should not be heated before mixing as this induces an oil to form. ***meso*-isomer**: mp 137–139 °C. ^1H NMR (250 MHz, DMSO-d_6): δ 8.69 (d, NH, 2 H), 8.58 (s, $C_6H_2O(NO_2)_3$, 4 H), 7.45 (m, C_6H_5, 5 H), 4.99 (q, CH_2CHNH, 2 H), 3.67 (s, $NHCH_2CH_2NH$, 8 H), 2.80, 1.98 (m, CCH_2CH_2CH, 8 H). ^{13}C [^1H] NMR (62.5 MHz, DMSO-d_6): δ 160.87, 159.40, 143.48, 141.81, 135.45, 134.30, 128.70, 128.22, 125.17, 124.29, 57.35, 42.61, 31.31, 26.74. Anal. Calcd for $C_{35}H_{33}N_{13}O_{14}\cdot 4H_2O$: C, 45.12; H, 4.43; N, 19.53. Found: C, 45.13; H, 3.56; N, 19.70. ***d,l* isomer**: mp 179–181 °C. ^1H NMR (250 MHz, D_2O): δ 8.69 (d, NH, 2 H), 8.58 (s, $C_6H_2O(NO_2)_3$, 4 H), 7.49 (m, C_6H_5, 5 H), 5.03 (q, CH_2CHNH, 2 H), 3.60 (s, $NHCH_2CH_2NH$, 8 H), 2.85, 2.60, 1.85 (m, CH_2CH_2, 8 H). ^{13}C [^1H] NMR (72.5 MHz, D_2O): δ 160.71, 159.21, 143.21, 141.81, 135.37, 134.02, 128.66, 128.33, 125.15, 124.23, 57.47, 42.59, 32.00, 26.67. Anal. Calcd for $C_{35}H_{33}N_{13}O_{14}\cdot 4H_2O$: C, 45.12; H, 4.43; N, 19.53. Found: C, 45.10; H, 3.53; N, 19.84.

***meso*- and *d,l*-*N,N'*-Bis(4,5-dihydro-1*H*-imidazol-2-yl)-1,2,3,5,6,7-hexahydro-8-phenyldicyclopenta[*b,e*]pyridine-3,5-diamine Dihydrochlorides 4.** IRA-100 ion-exchange resin in the OH^- form was equilibrated in 0.2 M HCl overnight. Approximately 4 mL of resin was packed in a 1-cm-diameter column and washed to neutrality with water. The dipicrate of **4** (300 mg) was dissolved in 300 mL of 50% acetonitrile in water. The solution was eluted slowly, and the effluent was collected in a 1-L round-bottom flask, evaporated to dryness, redissolved in a minimum amount of water, transferred to a smaller flask, and lyophilized. Yield: 135.1 mg (83.3%). ***meso* isomer**: mp 186–187 °C. ^1H NMR (250 MHz, D_2O): δ 7.45 (m, C_6H_5, 5 H), 4.9 (t, CH_2CHNH, 2 H), 3.62 (s, $NHCH_2CH_2NH$, 8 H), 2.75, 2.5, 1.9 (m, CH_2CH_2, 8 H). ^{13}C [^1H] NMR (72.5 MHz, D_2O): δ 160.50, 159.06, 148.76, 138.05, 136.06, 130.04, 129.60, 129.15, 58.14, 43.58, 32.49, 27.56. Anal. Calcd for $C_{23}H_{29}N_7Cl_2O$: C, 50.55; H, 6.81; N, 17.95. Found: C. 50.45; H, 6.20; N, 16.84. ***d,l* isomer**: mp 146–147 °C. ^1H NMR (250 MHz, D_2O): δ 7.33 (m, C_6H_5, 5 H), 4.97 (t, CH_2CHNH, 2 H), 3.59 (s, $NHCH_2CH_2NH$, 8 H), 2.74, 2.50, 1.83 (m, CH_2CH_2, 8 H). ^{13}C [^1H] NMR (72.5 MHz, D_2O): δ 160.89, 160.68, 145.77, 136.67, 136.43, 129.67, 129.60, 129.31, 119.99, 58.66, 45.94, 43.64, 32.55, 27.42. Anal. Calcd for $C_{23}H_{29}N_7Cl_2O\cdot 3H_2O$: C, 52.28; H. 6.66; N, 18.56. Found: C, 52.63; H, 6.33; N, 18.00.

***meso*- and *d,l*-*N,N'*-Bis(4,5-dihydro-1*H*-imidazol-2-yl)-1,2,3,5,6,7-hexahydro-8-phenyldicyclopenta[*b,e*]pyridine-3,5-diamine Dihydrotetraphenylborates 4.** Compound **4** dichloride (0.285 mmol, 135 mg) was dissolved in water and then combined with sodium tetraphenylboron (0.57 mmol, 222 mg, 2 equiv) also dissolved in water. A white precipitate formed immediately. The solution was stirred overnight and then lyophilized. A white powder was formed, which was dissolved in acetonitrile. Any additional sodium chloride was left undissolved and filtered off through Celite. ***meso* isomer**: mp 108–109 °C. ^1H NMR (250 MHz, D_2O): δ 7.43 (m, C_6H_5, 5 H), 7.30, 6.99, 6.83 (stt, TPB, 40 H), 4.85 (t, CH_2CHNH, 2 H), 3.62 (s, $NHCH_2CH_2NH$, 8 H), 2.86, 2.60, 1.96 (m, CH_2CH_2, 8 H). ^{13}C [^1H] NMR (72.5 MHz, D_2O): δ 164.65 (q), 161.18, 146.0, 136.6, 135.47, 129.77, 129.15, 125.57, 126.50, 122.70, 125.50. Anal. Calcd for $C_{71}H_{69}N_7OB$: C, 79.10; H, 6.82; N, 9.10. Found: C, 79.72; H, 6.72; N, 9.31. ***d,l* isomer**: mp 220–225 °C. ^1H NMR (250 MHz, CD_3CN): δ 7.63 (d, NH, 2 H), 7.42 (m, C_6H_5, 5 H), 7.28, 7.01, 6.82 (stt, TPB, 40 H), 4.88 (t, CH_2CHNH, 2 H), 3.65 (s, $NHCH_2CH_2NH$, 8 H), 2.75, 2.61, 1.9 (m, CH_2CH_2, 8 H). ^{13}C [^1H] NMR (72.5 MHz, CD_3CN): δ 165.17, 160.5, 146.00, 135.47, 129.71, 129.15, 126.56, 126.50, 122.76, 122.70, 125.5.

Determination of Binding Constants. All solutions were prepared in a drybox. A solution of sodium dibenzyl phosphate, henceforth called

the stock solution, of about 10 mM concentration was made, and the concentration was determined by UV-vis absorbance. The extinction coefficients at 255, 256, and 260 nm were 404, 437, and 377 M^{-1} cm^{-1}, respectively (determined by Beer's law plots). Approximately 80 mM host solution (550 μL) was made using the phosphate stock solution, and exactly 500 μL was transferred to a 5-mm NMR tube sealed with a septum. The dibenzyl phosphate resonance was observed as a single peak in the ^{31}P NMR. The chemical shift of pure dibenzyl phosphate in DMSO is δ 0.52 as referenced to phosphoric acid in D_2O. Aliquots of the host–guest solution were removed from the NMR tube via syringe through the septum and replaced by an equal volume of the guest stock solution. In this manner, the host concentration was systematically reduced while the guest concentration remained constant. The ratio of host to guest was determined by ^1H NMR integration.

The ^1H NMR binding studies followed the chemical shift of the amine protons of the host compounds when the solvent was pure DMSO. In DMSO/water mixtures, the methylenes of the imidazoline groups were monitored. A 5-mm NMR tube was fitted with a septum and charged with 500 μL of an approximately 3 mM solution of host, and small aliquots (1–5 μL) of a guest stock solution of approximately 100 mM were added. The binding constants were obtained by using a curve-fitting program provided by Dr. Howard Whitlock of The University of Wisconsin.

X-ray Crystallography. Crystals of $(C_{23}H_{29}N_7)^{2+}(C_6H_5PO_4)^{2-}\cdot H_2O$ [*meso*-**4**$(C_6H_5PO_4)^{2-}\cdot H_2O$] were grown from H_2O–DMF solution as long, colorless crystals, while crystals of $(C_{23}H_{29}N_7)^{2+}(C_{14}H_{14}OPO_3)^-\cdot H_2O$ [*meso*-**4**$(C_{14}H_{14}OPO_3)^-(Cl)^-\cdot H_2O$] were grown from H_2O–DMSO solution, also as long, colorless needles. Data for both were collected on a Nicolet P3 diffractometer with a graphite monochromator, using Mo Kα radiation (λ = 0.71073 Å). Details of the crystal data, data collection, and structure refinement are listed in the supplementary material, Table 1. The data for *meso*-**4**$(C_6H_5PO_4)^{2-}\cdot H_2O$ were collected from 4.0° to 47.5° in 2θ using the ω scan technique, with a 1.2° scan range in ω at 2.5–5° min^{-1}. A total of 6680 reflections were measured, of which 4565 were unique (R for averaging equivalent reflections = 0.019). It was apparent from the initial photographs of the data crystal that it was limited in scattering power, and therefore, the data were collected in two stages. For the first stage, a quadrant of the reciprocal lattice was collected out to a 2θ maximum of 47.5° where h ranged from 0 to 12, k ranged from 0 to 10, and l ranged from −36 to 36. A second stage was collected out to a 2θ maximum of 30° to give some redundancy to that part of the data set most likely to be observable. Three reflections (1, 0, 8; 2, 1, −3; and −2, −1, −3) were remeasured every 97 reflections to monitor instrument and crystal stability. A smoothed curve of the intensities of these check reflections was used to scale the data. The scaling factor ranged from 0.982 to 1.01. The data for *meso*-**4**$(C_{14}H_{14}OPO_3)^-(Cl)^-\cdot H_2O$ were collected from 4.0° to 50° in 2θ using ω scan technique, with a 1.2° scan range in ω at 3–6° min^{-1}. Two complete equivalent sets of data were collected. A total of 10 516 reflections were measured, of which 6545 were unique (R for averaging equivalent reflections = 0.026) where h ranged from −21 to 20, k ranged from 0 to 12, and l ranged from −23 to 23. Four reflections (−2, 2, 4; 3, 0, 4; 1, −3, −1; and −1, 2, −3) were remeasured every 96 reflections to monitor instrument and crystal stability. A smoothed curve of the intensities of these check reflections were used to scale the data. The scaling factor ranged from 0.991 to 1.01. The data for both samples were corrected for L_p effects and absorption. The absorption correction was based on measured crystal faces. Data reduction and decay correction were performed using the SHELXTL-*Plus* software package.[38] The structures were solved by direct methods and refined by full-matrix least squares[38] with anisotropic thermal parameters for the non-H atoms. For *meso*-**4**$(C_6H_5PO_4)^{2-}\cdot H_2O$, the hydrogen atoms were located from a ΔF map and refined with isotropic thermal parameters. For *meso*-**4**$(C_{14}H_{14}OPO_3)^-(Cl)^-\cdot H_2O$, hydrogen atoms, except for those on the water molecules, were calculated in ideal positions (C–H, 0.96 Å and N–H, 0.90 Å) with U_{iso} fixed at $1.2U_{eq}$ of the relevant atom. Positions for the hydrogen atoms on the water molecules were located from a ΔF map and were tied to the water oxygen atom during least squares. The function $\sum w(|F_o| - |F_c|)^2$ was minimized, where $w = 1/(\sigma(F_o))^2$ and $\sigma(F_o) = 0.5kI^{-1/2}[(\sigma(I))^2 + (0.02I)^2]^{1/2}$. The intensity I is given by $(I_{peak} - I_{background})$(scan rate), where 0.02 is a factor to down-weight intense reflections and to account for instrument instability and k is the correction due to Lp effects, absorption, and decay. $\sigma(I)$ was estimated from counting statistics; $\sigma(I) = (I_{peak} + I_{background})^{1/2}$(scan rate). Neutral atom scattering factors for the non-H atoms were taken from Cromer and Mann,[39] with the anomalous-dispersion corrections taken from the work of Cromer and Liberman.[40] The scattering factors for the H atoms were obtained from Stewart, Davidson, and Simpson.[41] Values used to calculate the linear absorption coefficients are from *International Tables for X-ray Crystallography* (1974).[42] All figures were generated using SHELXTL-*Plus*.[1] Other computer programs used in this work are listed elsewhere.[43]

Acknowledgment. We gratefully acknowledge financial support for this project from the Searle Foundation (Chicago Community Trust) and an NSF-PYI award to E.V.A. We also thank Professor Craig Wilcox of The University of Pittsburgh for helpful discussions related to the fitting of 2:1 NMR titration data. In addition, we thank Ryan Breed and Clarence Johnson for assistance with syntheses.

Supplementary Material Available: X-ray experimental summary, positional and thermal parameters, bond lengths and angles, listing of the H-bonding interactions, view showing the atom-labeling schemes, and unit cell packing diagrams along with some additional superposition plots of the tricyclic ring system of *meso*-**4**$(C_6H_5PO_4)^{2-}\cdot H_2O$ fitted by *meso*-**4**$(C_{14}H_{14}OPO_3)^-(Cl)^-\cdot H_2O$ (48 pages); tables of observed and calculated structure factor amplitudes (41 pages). Ordering information is given on any current masthead page.

(38) Sheldrick, G. M. SHELXTL-*Plus* (version 4.11). Siemens X-ray Analytical Instruments, Inc.: Madison, WI, 1991.
(39) Cromer, D. T.; Mann, J. B. *Acta Crystallogr. Ser. A* **1968**, *24*, 321–324.
(40) Cromer, D. T.; Libermann, D. *J. Chem. Phys.* **1970**, *53*, 1891–1898.
(41) Stewart, R. F.; Davidson, E. R.; Simpson, W. T. *J. Chem. Phys.* **1965**, *42*, 3175–3187.
(42) *International Tables for X-ray Crystallography*; Kynoch Press: Birmingham, 1974; Vol. IV, p 55.
(43) Gadol, S. M.; Davis, R. E. *Organometallics* **1982**, *1*, 1607–1613.